

# Study of the Nucleon Spin Structure in Strong and Electromagnetic Interactions

Project "GDH & SPASCHARM & NN"

Dubna—Protvino—Prague—Moscow—Mainz—Glasgow—Los  
Angeles—Basel—Lund—Zagreb—Pavia—Lund—Kharkov—Bochum  
Bonn—Amherst—Giessen—Halifax—Jerusalem—Kent—Regina—Sackville  
Washington—York

Dubna

2022

**Study of the Nucleon Spin Structure in Strong and  
Electromagnetic Interactions**

**Project "GDH & SPASCHARM & NN"**

**THEME 04-2-1126-2015/2025**

Dubna, Dzheleпов Laboratory of Nuclear Problems, JINR  
N.A. Bazhanov, N.S. Borisov, A.S. Dolzhikov, A.N. Fedorov, I.V.  
Gapienko, I. Gorodnov, G.M. Gurevich, V.L. Kashevarov, A.  
Kovalik, E.S. Kuzmin, A.B. Lazarev, A.B. Neganov, Yu.A. Plis, A.A.  
Priladyshev, A.B. Sadovski, Yu.A. Usov, Yu.N. Uzikov, V.P. Volnykh

Dubna, Bogoliubov Laboratory of Theoretical Physics, JINR  
S.B. Gerasimov

NRC "Kurchatov Institute" - IHEP, Protvino, Russia  
V.V. Abramov, A.A. Derevschikov, V.I. Garkusha, A.P. Meschanin,  
V.V. Mochalov,  
V.V. Moiseev, D.A. Morozov, L.V. Nogach, A.F. Prudkoglyad, A.V.  
Ryazantsev,  
S.V. Ryzhikov, P.A. Semenov, A.N. Vasiliev, V.N. Zapolsky, A.E.  
Yakutin

NRC "Kurchatov Institute" - ITEP, Moscow, Russia  
I.G. Alekseev, V.M. Nesterov, D.N. Svirida

National Research Nuclear University MEPhI, Moscow, Russia  
M.B. Nurusheva, V.A. Okorokov, V.L. Rykov

Institute for Nuclear Research, Russian Academy of Science,  
Moscow, Russia

G.M. Gurevich, R.L. Kondratiev

IEAP, CTU, Prague, Czech Republic

J. Černý, Z. Janout, Z. Kohout, J. Koniček, J. Petrík, S. Pospíšil,  
R.Sykura, M. Solar, I. Štekl, J. Šveida, I. Wilhelm,

Institut für Kernphysik, Universität Mainz, Mainz, Germany

M. Biroth, A. Denig, V.L. Kashevarov, M. Ostrick, E.-P. Schilling, A.  
Thomas

Helmholtz-Institut für Strahlen- und Kernphysik, Universität Bonn,  
Germany

R. Beck, H. Dutz, J. Hartmann, M. Lang, S. Runkel, U. Thoma

Institut für Experimentalphysik I, Ruhr-Universität, Bochum,  
Germany

W. Meyer, G. Reichers

University of Giessen, D-35392 Giessen, Germany

V. Metag, M. Nanova

Kharkov Institute of Physics and Technology, Kharkov, Ukraine

A.A. Belyaev, A.A. Lukhanin

MAX-lab., Lund University, Lund, Sweden

K. Hansen, L. Isaksson, B. Schröder

University of Basel, Ch-4056 Basel, Switzerland

B. Krushe, N.K. Walford

University of Glasgow, Glasgow, UK

J.R.M. Annand, D.I. Glazier, K. Livingston, I.J.D. MacGregor

University of York, Heslington, York, UK  
M. Bashkanov, D.P. Watts, D. Werthmüller

Saint Mary's University, Halifax, Canada  
A. Sarty

University of Regina, Regina, Canada  
G.M. Huber

Mount Allison University, Sackville, Canada  
D. Hornige

Hebrew University of Jerusalem, Jerusalem Israel  
G. Ron

Kent State University, Kent, USA  
D.M. Manley

University of Massachusetts, Amherst, USA  
R. Miskimen

The George Washington University, Washington, USA  
W.J. Briscoe, E.J. Downie, I.I. Strakovsky

University of California Los Angeles, USA  
S.N. Prakhov

INFN Sezione di Pavia, Pavia, Italy  
A. Braghieri, P. Pedroni

**Rudjer Boskovic Institute, Zagreb, Croatia**  
**M. Korolja, I. Supek**

Leaders of the Project A. Kovalik, Yu.A. Usov

Deputies of the Leaders Yu.A. Plis, Yu.N. Uzikov

DATE OF THE PROJECT PRESENTATION IN SO & IC

DATE OF LABORATORY STB      NUMBER OF DOCUMENT

DATE OF THE BEGINNING OF THE PROJECT

(FOR PROLONGATION - DATE OF FIRST APPROVAL OF THE PROJECT)

ЛИСТ СОГЛАСОВАНИЙ ПРОЕКТА

**Изучение спиновой структуры нуклонов в сильных и электромагнитных взаимодействиях**

**Study of the Nucleon Spin Structure in Strong and Electromagnetic Interactions**

**GDH & SPASCHARM & NN**

04-2-1126-2015/2020

Руководители Проекта: Алоиз Ковалик, Юрий Андреевич Усов

УТВЕРЖДЕН ДИРЕКТОРОМ ОИЯИ	ПОДПИСЬ	ДАТА
СОГЛАСОВАНО		
ВИЦЕ-ДИРЕКТОР ОИЯИ	ПОДПИСЬ	ДАТА
ГЛАВНЫЙ УЧЕНЫЙ СЕКРЕТАРЬ	ПОДПИСЬ	ДАТА
ГЛАВНЫЙ ИНЖЕНЕР	ПОДПИСЬ	ДАТА
НАЧАЛЬНИК НОО	ПОДПИСЬ	ДАТА
ДИРЕКТОР ЛАБОРАТОРИИ	ПОДПИСЬ	ДАТА
ГЛАВНЫЙ ИНЖЕНЕР ЛАБОРАТОРИИ	ПОДПИСЬ	ДАТА
РУКОВОДИТЕЛИ ПРОЕКТА	ПОДПИСЬ	ДАТА
ЗАМ. РУКОВОДИТЕЛЕЙ ПРОЕКТА	ПОДПИСЬ	ДАТА
ОДОБРЕН		
ПКК ПО ЯДЕРНОЙ ФИЗИКЕ	ПОДПИСЬ	ДАТА

# Contents

<b>1</b>	<b>Introduction</b>	<b>7</b>
<b>2</b>	<b>SPASCHARM</b>	<b>10</b>
2.1	Single-spin asymmetries in light resonance production . . . . .	12
2.2	Charmonium production in polarized $p \rightarrow p \rightarrow$ interactions . . . . .	14
2.3	Polarized frozen-spin target at Protvino . . . . .	15
2.4	Main results . . . . .	17
<b>3</b>	<b>GDH: Helicity dependence of single and double pion photoproduction processes and the GDH integral on the neutron</b>	<b>17</b>
3.1	Physics motivations . . . . .	19
3.2	The GDH sum rule on the neutron . . . . .	19
3.3	Helicity dependence of meson photoproduction on the proton . . . . .	23
3.4	Measurement of the $G$ asymmetry in $\vec{\gamma}\vec{p} \rightarrow p\pi^0$ and $\vec{\gamma}\vec{p} \rightarrow n\pi^+$ . . . . .	24
3.5	Transverse asymmetries $T$ and $F$ in $\eta$ photoproduction in the $S_{11}(1535)$ region . . . . .	25
3.6	Spin observables for $\pi\eta$ photoproduction in the $D_{33}(1700)$ region . . . . .	25
3.7	Measurement of polarized target and beam asymmetries in pion photo-production on the proton: test of chiral dynamics . . . . .	25
3.8	Measurement of the proton spin polarizabilities . . . . .	26
3.9	Photoproduction of pions off polarized neutrons . . . . .	26
3.10	Polarized frozen-spin target at Mainz . . . . .	27
	3.10.1 Refrigerator . . . . .	28
	3.10.2 Polarizing magnet . . . . .	29
3.11	Main results . . . . .	30
3.12	CBELSA-Bonn . . . . .	33
3.13	P2MESA-Mainz . . . . .	35
<b>4</b>	<b>NN-interactions</b>	<b>37</b>
4.1	Motivation . . . . .	37
4.2	Experiments . . . . .	38
4.3	Former experiments at Prague . . . . .	39
4.4	Proposed experiments at Prague . . . . .	40
4.5	Polarized deuterons . . . . .	42
4.6	Experimental setup . . . . .	43
4.7	Neutron beam . . . . .	46
4.8	Statistical error . . . . .	47
4.9	Main results . . . . .	47
<b>5</b>	<b>Working plan: 2023 - 2024 - 2025</b>	<b>47</b>

# 1 Introduction

The dependence of the nuclear interactions on spins of involved particles is an object of the polarization studies. The concept of spin had been introduced into science almost 100 years ago for the description of atomic spectra, but its nature stays an unresolved mystery until now. The appearance of the experimental polarization data stimulated theoretical comprehension of spin phenomena and turned up the testing ground for theoretical models. However, the subject appeared to be so difficult that once the leading theorist in the field, Elliot Leader, pronounced in desperation "Experiments with spin have killed more theories than any other physical parameter" (Elliot Leader. *Spin* in Particle Physics, Cambridge U. Press (2001)). Another famous statement of this kind was from James Bjorken: «Polarization data has often been the graveyard of fashionable theories. If theorists had their way they might well ban such measurements altogether out of self-protection» (J.D.Bjorken. Proc. Adv. Workshop on QCD Hadronic Processes, St. Croix, Virgin Islands, 1987). Today there is no theory which provides a complete and consistent description of all observed polarization effects in the hadron sector. Therefore, the systematic experimental study of polarization effects in a wide variety of reactions, using polarized beams and polarized targets, is of great importance for development of a theory for the consistent description of all observed spin phenomena.

Polarization observables are paramount characteristics of elementary particle interactions and nuclear reactions. Formally, the measurement of spin-dependent parameters inflicts additional limitations on the presumed reaction mechanism, investigated micro-object structure and the fundamental interaction character itself. It should be mentioned that modern experiments aimed at the search of CP-invariance and T-invariance violation effects outside the standard model, as well as CPT-symmetry violation, are based on the polarization measurements.

Due to the complexity of polarization experiments this area began to evolve dynamically comparatively recently, in accordance with the progress of experimental technique. Nowadays, almost all modern accelerators of protons, deuterons and electrons produce polarized beams and have programs of polarization experiments. The targets of polarized protons, deuterons,  $^3\text{He}$  and heavier nuclei are developed actively. High-density gas polarized targets (storage cells) used at the storage rings are in progress. The advanced track devices are developed which allow to build effective and fast polarimeters. This technical progress makes now accessible more and more intricate polarization measurements.

The vast scope of experimental data on nuclear reaction cross sections accumulated during the decades of measurements appears nonetheless not exhaustive without taking into consideration the dependence on spins of the interacting particles. Only polarization experiments permit to evolve all independent amplitudes describing the specific reaction. In other words, only polarization measurements allow to obtain a complete information about any physical process under study.

Theoretical and experimental studies in this field are traditional for JINR [1]. In recent years, the improvements in experimental methods have opened up new opportunities for the investigation of the polarization degrees of freedom of the nucleon.

This project covers three spin physics problems:

- 1) Experimental study of single-spin asymmetries in the production of miscellaneous light particles with the use of 28 GeV  $\pi^-$ -beam at first stage and the study of single-spin and



double-spin asymmetries in charmonium production with the use of polarized proton beam (SPASCHARM project).

The ultimate goal of the SPASCHARM project is to study spin structure of the proton, starting with determination of gluon contribution into the proton spin at large values of the Bjorken variable  $x$  through a study of spin effects in charmonium production. This will allow to understand charmonium hadronic production mechanism and to extract gluon polarization  $\Delta g(x)$  at large  $x$ .

2) Experiments with a real photon beam: meson photoproduction on nucleons and nuclei and Compton scattering on nucleons. The main goals: experimental verification of the Gerasimov-Drell-Hearn (GDH) sum rule, investigation the helicity structure of partial reaction channels, resolve the excitation spectrum of light-quark baryons, search for missing baryon resonances and exotic states (dibaryons, narrow nucleon resonances), studying the structure of hadrons.

3) Measurement of  $\Delta\sigma_T$  and  $\Delta\sigma_L$  in the nd transmission experiment at neutron energies  $\leq 16$  MeV where limited experimental data exist and where the theory predicts the essential effect of the 3NF. This part of the project is the continuation of the same quantities measurements in neutron-proton scattering being performed previously.

Technically, three parts of the project are unified by the use of the frozen-spin polarized proton and deuteron targets.

1) High sensibility to gluon content of the interacting particles is one of the main features of charmonium production in hadronic interactions. In case of collision of two longitudinally polarized protons it is used to define gluon polarization  $\Delta G/G$  in the proton. A polarized proton beam is needed to make this study. It will be used at the second stage of the experiment after the completion of measurements of single-spin asymmetries in charmonium production.

At the first stage unpolarized beams will be used. The first stage envisages a study of the single-spin asymmetry  $A_N$  of light resonances consisting of  $u$ -,  $d$ - and  $s$ -valence quarks. Transverse single-spin asymmetries are very well known for a long time. In the Standard Model QCD at leading twist level all  $A_N = 0$ . But the experiments show very large  $A_N$  in the confinement region. To discriminate the existing theoretical approaches and to stimulate the development of the new ones, a systematic study of  $A_N$  for a big number of miscellaneous inclusive and exclusive reactions is needed, especially in the confinement region, which is the most unclear for theory. This systematic study is the main goal of the first stage of the SPASCHARM project. The first stage will be finalized by the measurements of  $A_N$  in charmonium production. This will finally prepare the experimental setup to the second stage of the project where only one new thing will be needed — namely a polarized proton beam from U70.

2) The MAInz MIcrotron at the Institute for Nuclear Physics at the Johannes Gutenberg University was built in 1979. The first stage was MAMI-A1 where the exploitation of the microtron principle led to a maximum electron energy of 14 MeV. It was followed by MAMI-A2 in 1983 when the 183 MeV facility was put into operation. In 1991 MAMI-B was completed, producing electrons up to 855 MeV.

MAMI-B is a continuous wave electron accelerator with 100% duty cycle, a maximum

current of  $100 \mu\text{A}$  and maximum energy of 855 MeV. A 3.5 MeV LINAC injects the electrons into a cascade of 3 Race Track Microtrons (RTM). The LINAC is fed either with 100 keV unpolarized electrons from a thermionic source, or with linearly polarized electrons originating from a  $\text{GaAs}_{0.95}\text{P}_{0.5}$  crystal photo-cathode which is irradiated by circularly polarized 830 nm laser light from a Titanium-Sapphire laser. The maximum current of the polarized source is  $30 \mu\text{A}$  with a degree of polarization of (75 – 82)%. During the experiment the direction of the polarization is changed every second in order to reduce systematic errors.

In 2006 the beam energy of Mainz electron accelerator has been increased from 855 MeV (MAMI-B) to 1604 MeV (MAMI-C) while preserving the outstanding beam quality. The photon tagger system of A2 collaboration was accordingly upgraded to make use of the extended energy range and provides now energy-marked circularly polarized photons with the maximum energy over 1550 MeV. In order to tag the high energy part of the bremsstrahlung spectrum, a dedicated end-point tagging spectrometer was developed. It is specially important for the measurement of  $\eta'$  meson-photoproduction. Using a diamond crystal as a radiator allows to obtain linearly polarized photons.

To realize the program of double polarization experiments, the new frozen spin polarized target facility had been developed which was put into operation in the end of 2009. This facility allows obtaining of longitudinally or transversely polarized protons and neutrons (using butanol or deuterated butanol as a target material). An addition of thin internal superconducting holding coils (solenoid or saddle-shaped) to support target polarization in the frozen spin mode allows to use the target in combination with  $4\pi$  detecting system of A2 collaboration including the Crystal Ball detector complemented by the TAPS detector for forward angles. Unusually low working temperature of the target cryostat (below 30 mK) provides a polarization relaxation time of many hundreds of hours (up to 2000 hours). As a consequence, during measurements the target repolarization is required only once or twice a week which makes the data taking more effective.

Program of experiments is directed at the study of various aspects of the QCD spin-flavor structure of the nucleons. It includes the verification of Gerasimov-Drell-Hearn (GDH) sum rule for proton and neutron in a wider energy range. Precise measurements of the helicity asymmetry of meson photoproduction with different final states (including neutral ones) will give more detailed information on nucleon resonance properties and multipole amplitudes. Measurements using different combinations of beam and target polarizations will allow the determination of polarization observables with high quality. An extraction of the spin polarizabilities of nucleons from experimental data is also envisaged.

The multipole analysis of the obtained experimental data with the help of the gradually improving MAID package [2] provides a firm basis for a theoretical treatment. The last modification of the package [3] is already available on-line: <https://maid.kph.uni-mainz.de/eta2018/etamaid2018.html>. Presently there is also an intense theoretical activity to improve and optimize various calculational schemes including the Lattice QCD and the Chiral Perturbation Theory.

3) The problem of nuclear force is one of the oldest but still most essential problems in nuclear physics. It is of crucial importance for understanding the properties of atomic nuclei and, more generally, strongly interacting hadronic matter. The conventional way to describe the nuclear force utilizes the meson-exchange picture, which goes back to the work by Yukawa [4]. His idea, followed by the experimental discovery of  $\pi$ - and heavier mesons ( $\rho$ ,  $\omega$ , ...), stimulated

the development of boson-exchange models that have laid the foundations for the construction of phenomenological nucleon–nucleon (NN) potentials.

In a first approximation, the two-nucleon potential is sufficient to describe the bulk of the few-nucleon observables at low and intermediate energies. At present, a number of semiphenomenological two-nucleon models is available which provide an accurate description of the NN scattering data below the pion-production threshold. Recent advances in the development of few-body methods coupled with a significant increase in computational resources allow one to perform accurate microscopic calculations of three- and even four-nucleon scattering observables and of the spectra of light nuclei. This opens the door for precise tests of the underlying dynamics and, in particular, of the role and structure of the three-nucleon forces (3NF).

## 2 SPASCHARM

At the largest accelerator in Russia, the U-70, of the National Research Center Kurchatov Institute (NRC KI) - IHEP, Protvino a significant base for conducting world class research in the fixed target SPASCHARM experiment (SPin ASymmetry in CHARMonia) has been created [5]. These studies will allow the NRC KI to take the world’s leading positions in the field of spin physics.

The project is aimed at studying the spin structure of the nucleon and the spin dependence of the strong interaction of antimatter and matter with matter at energies up to 50 GeV. Spin was introduced almost 100 years ago in order to describe atomic spectra. Its nature is still an unsolved mystery. The SPASCHARM project intends to become a breakthrough in the fundamental science which will bring closer the understanding of the spin mystery. Spin-dependence of fundamental interactions represents the essence of polarization phenomena. In order to carry out polarization studies in collisions of high-energy particles, it is necessary to create beams of polarized particles and/or to use the technique of polarized targets. In recent years, there has been noticeable progress in the experimental studies of spin effects at high energies. The overwhelming majority of experiments have been carried out in the kinematic region of nonperturbative quantum chromodynamics (QCD) at moderate momentum transfers. These experimental data stimulated the development of theory on the spin role in physics of strong interactions. Therefore, the systematic experimental study of polarization effects in a wide variety of reactions, including antiproton-proton and proton-proton collisions, is of great importance for development of a theory for the consistent description of all observed spin phenomena in QCD nonperturbative region.

It is proposed to form polarized beams of protons and antiprotons in the beamline 24A of the accelerator U-70 [6] (Fig. 1). Calculations of their parameters have been carried out.

The intensity of the antiproton beam with energy of 16 GeV can reach  $10^6$  antiprotons per accelerator cycle ( $10^{10}$  antiprotons per day) for the  $10^{13}$  primary protons from the U-70 to the primary target. A polarized antiproton beam from the decay of the anti-lambda hyperons, which can be reached by NRC KI in 2022, will certainly be a unique beam in the world. In antiproton-proton annihilations there is no restriction on the quantum numbers of the majority of the producing resonances. The intensity of a polarized proton beam with energies of 10 – 45 GeV will be an order of magnitude larger than that of an antiproton beam with the same mean polarization.

All this will allow the SPASCHARM setup to solve large-scale scientific problems related to spin. There is no closest analogue of the new fixed target SPASCHARM complex being created for operation on polarized beams. The expected period of preserving the uniqueness of the SPASCHARM complex is no less than fifteen years. Polarized beams will be a powerful tool for carrying out systematic polarization studies. These studies will be carried out on antiproton and proton beams at an energy of 16 GeV and above, with an average polarization of 45%. At the first stage unpolarized beams will be used. The first stage envisages a study of the single-spin asymmetry  $A_N$  of light particles consisting of  $u$ -,  $d$ - and  $s$ -valence quarks. Transverse single-spin asymmetries are very well known for a long time. In the Standard Model QCD at leading twist level all  $A_N$  are small or close to zero. But the experiments show very large  $A_N$  (up to 40 %) in the confinement region. To discriminate the existing theoretical approaches and to stimulate the development of the new ones, a systematic study of  $A_N$  for a big number of miscellaneous inclusive and exclusive reactions is needed, especially in the confinement region, which is the most unclear for theory.

It is planned to determine a large set of necessary physical observables, including single-spin asymmetries in dozens of reactions in the region of fragmentation of a polarized beam, both on hydrogen and on various nuclear targets. Data in this volume are absent at any energy. The results of the comparison will point to the difference between the interaction of antimatter and matter with matter, which has been an actual scientific task for many years. To study the spin structure of the nucleon, studies will be made of the formation of charmonium in the fragmentation region of a polarized beam, with an emphasis on determining the contribution of gluons to the proton spin, which will help solve the "spin crisis" of the proton (all quarks in the proton are responsible for only  $\sim 30\%$  of the proton spin) existing already almost 30 years.

The presence of polarization for both protons and antiprotons in the CP neutral  $p\bar{p}$ -system potentially opens up opportunities for studying and comparing CP conjugate reactions in this system. It allows us to look at CP invariance in a new perspective, inaccessible to collisions of unpolarized particles. It is interesting that the LHCb collaboration has just presented at the Rencontres de Moriond EW and in a special CERN Seminar the first observation of CP violation in charm particle decays. The final result, which uses essentially the full data sample collected by LHCb so far, is given by the quantity  $\Delta A_{CP} = (-0.154 \pm 0.029)\%$ , whose difference from zero quantifies the amount of CP violation observed [7].

Additional unique features of the SPASCHARM experiment are associated with the possibility of measuring the multiplicity of charged hadrons in an event, determining the centrality of the hadron-nucleus collisions. There have been almost no such studies in the world, but there are first indications of their relevance. Another novelty of the project is connected with the possibility to register not only stable particles that are stable by strong interaction, but also numerous resonances, both meson and baryon ones. In the SPASCHARM setup, it is also possible to measure the transverse polarization of hyperons and the elements of the spin matrix of vector mesons, which is a huge advantage of the project. Finally, the presence of eight types of unpolarized beams ( $\pi^\pm$ ,  $K^\pm$ , p,  $\bar{p}$ , d, C), in combination with a polarized target, extends the range of studies of polarization phenomena by an order of magnitude and enhances the uniqueness of the project. The study of energy dependence of spin effects reveals the dynamics of interaction. The measurements might be conducted at several energies in order to estimate the model parameters.

The SPASCHARM polarization project is distinguished by a global, systematic approach

to the study of the antiproton-proton (nuclei) and proton-proton (nuclei) systems. Unlike most fixed target polarization experiments, in the wide-aperture precision spectrometer SPASCHARM, the full geometry along the azimuthal angle will be realized, which will allow us to investigate dozens of new processes with extremely low errors. The combination of a wide range of beams and targets with the possibility of simultaneous detection of charged and neutral particles in final states of reactions distinguishes this project from other polarization projects intended for a study of only limited number of reactions. Measurement of spin effects in a large kinematic range in the beam fragmentation region and comparison of spin effects in various reactions are of fundamental importance for revealing the mechanism of particle interaction. The core of the team of authors of this project is the laboratory of polarization experiments of IHEP. This team has a large scientific background on the project, both in terms of the scientific part and the equipment prepared. It has been engaged in polarization studies for more than 40 years and has been involved practically in all of the largest hadronic experiments on spin topics in Russian and foreign scientific centers. In particular, the team played a decisive role in the preparation and conduct of polarization experiments at FNAL (experiments E-581 and E-704) and BNL (spin part of STAR and E-925). In experiments conducted in Protvino and foreign centers, significant polarization effects were found that can't be explained by existing theoretical models.

Strategies of the SPASCHARM experiment:

Stage 1. Single-spin asymmetry on the beamline 14 (2018-2024) [8], including the first measurements of polarization and buildup.

Stage 2. Creation of the polarized proton and antiproton beams (research is planning to be started in 2024-2025):

Systematic study of inclusive, exclusive and elastic reactions in the production of the particles consisting of light quarks (u, d, s).

Polarization (buildup) in the processes of a production of hyperons and vector mesons.

The high accuracy study of the beam particle type, plurality and atomic number dependence from kinematic parameters ( $0 < x_F < 1$ ,  $0 < p_T < 3.0$ ,  $12 < E_{beam} < 60$  GeV) in total azimuth angle range and with wide aperture.

Double-spin asymmetry  $A_{ll}$  in the production of charmonium for the study of the gluon contribution  $\Delta G/G(x)$  into proton spin at big  $x_F$ .

## 2.1 Single-spin asymmetries in light resonance production

It would be interesting to measure single-spin asymmetries in inclusive production of light resonances even in the unpolarized beam fragmentation region, but at big values of transverse momentum  $p_T$ , close to the boundary of phase space. In the inclusive reaction  $\pi^- + d \uparrow \rightarrow \pi^0 + X$  at 40 GeV/c and  $x_F > 0.7$  the single-spin asymmetry  $A_N$  is zero at small  $p_T$  and about 15% at  $p_T$  near 1 GeV/c and bigger [9]. When  $x_F$  goes to 1, any inclusive reaction transfers into the proper exclusive reaction. In the exclusive reaction  $\pi^- + p \uparrow \rightarrow \pi^0 + n$  at 40 GeV/c the single-spin asymmetry  $A_N$  is also about 15% near  $-t$  equal to 1 (GeV/c)<sup>2</sup>, that is equivalent to  $p_T$  near 1 GeV/c [10]. So asymmetries in both inclusive and exclusive  $\pi^0$ -production at 40 GeV pion beam are equal each other (also it seems that asymmetries on polarized protons and neutrons are the same). It should be the case for other light resonances. For the first stage

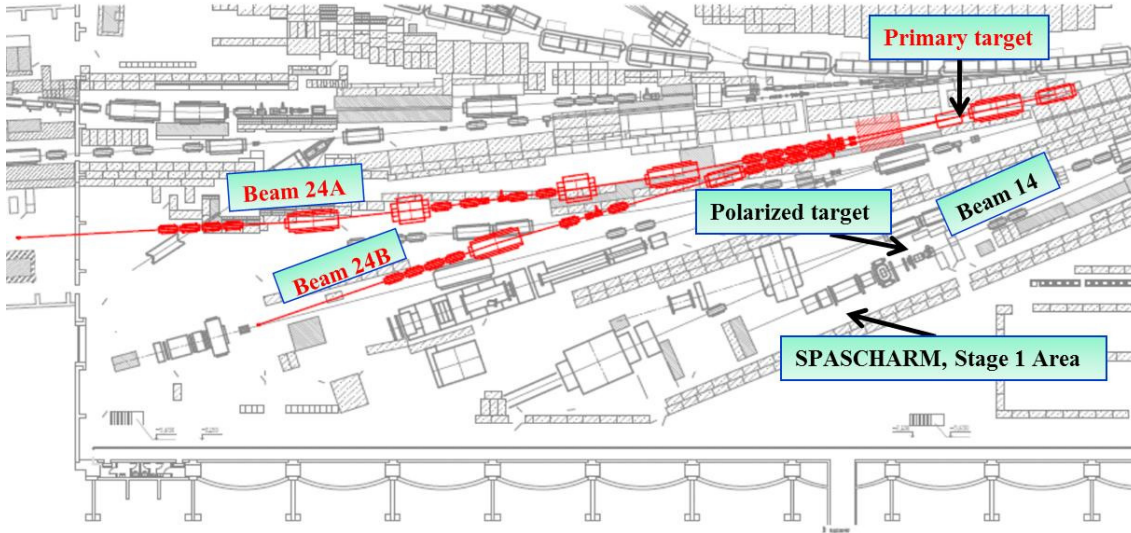


Figure 1: Scheme of beamlines 24A and 24B in the experimental hall of the U70.

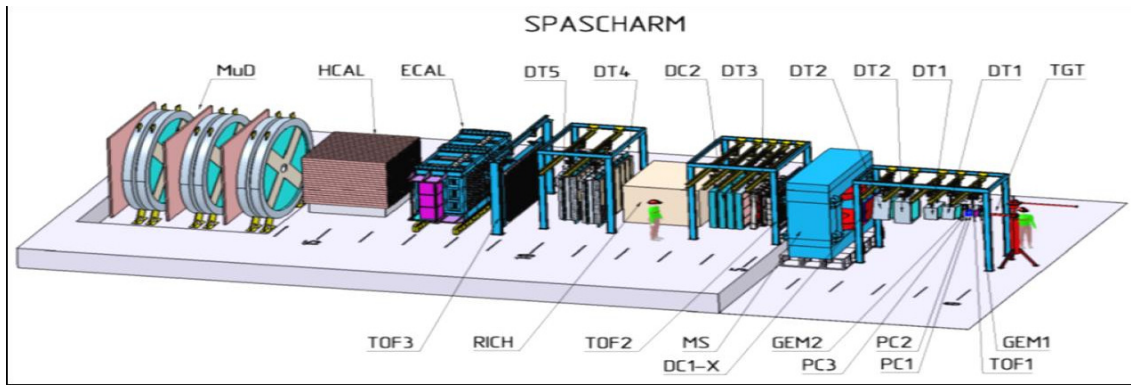


Figure 2: SPASCHARM experimental setup.

of the experiment two multi-channel threshold Cherenkov counters will be added to the setup to distinguish between pions and kaons. They are of 1.5 m and 3 m long and will be placed between the end of the magnet and the calorimeter. They will be filled with freon and with air correspondingly, both at atmospheric pressure. Lead tungstate in the calorimeter is not needed for the first stage, lead glass with moderate energy resolution will be enough to detect light resonances. An acceptance of the whole setup will be decreased, however it will still be significant to detect light resonances.

There are some advantages of the new experiment. Exclusive and inclusive reactions were studied either in neutral decay modes or in charged decay modes in the previous experiments. We propose to measure both modes simultaneously and therefore we expect a significant increase in statistics. At the PROZA facility, substantial asymmetries (up to 30-40%) and oscillations were fixed in some reactions with photons in final state. The increase of statistics approximately on the order of value is anticipated in the reactions  $\pi^- p \uparrow \rightarrow \omega(782)n$  and  $\pi^- p \uparrow \rightarrow \eta'(958)n$  and also as much as a factor of 3-4 in the reactions  $\pi^- p \uparrow \rightarrow f_2(1270)n$  and  $\pi^- p \uparrow \rightarrow a_2(1320)n$ . Firstly, there will be measured the asymmetry in the reaction  $\pi^- p \uparrow \rightarrow a_0(980)n$  when  $a_0(980)$

decays to  $\eta(550)$  and  $\pi^0$  (the expected effect is more than 50%).

Partial wave analysis of a huge statistics on polarized target will increase a robustness of the results on rare resonances. The setup has  $2\pi$ -acceptance on azimuthal angle  $\phi$  and therefore the systematic errors in single-spin asymmetries will be negligible.

## 2.2 Charmonium production in polarized $p \rightarrow p$ interactions

Double-spin effects in dozens of reactions will be measured with the use of polarized target and beam (proton and antiproton) to investigate spin dynamics and proton spin structure. The ultimate goal is to measure gluon contribution in the model independent approach. At present only 30% of the longitudinally polarized proton spin is described by quark's spin. The other 70% of the proton spin may be explained by gluon and/or orbital momentum contributions. Experiments with polarized lepton beams at CERN, HERA, SLAC have been measuring mainly quark polarization over last twenty years. COMPASS and HERMES have tried to measure gluon polarization at small  $x$ , up to 0.1–0.15. The RHIC experiments STAR and PHENIX have begun to measure gluon polarization at very low  $x$  values (about 0.01) whereas gluon polarization has to be measured in the whole  $x$  range. So, in spite of many years of experiments, a detailed decomposition of the spin of the proton remains elusive — new experimental data on  $\Delta g(x, Q^2)$ , especially at large  $x$  are badly needed. We propose to measure simultaneously the double-spin asymmetry  $A_{LL}$  for inclusive  $\chi_{c2}$ ,  $\chi_{c1}$  and  $J/\Psi$  by utilizing the 45 GeV longitudinally polarized proton beam on a longitudinally polarized target. Our goal is to obtain besides the quark-spin information also the gluon-spin information from these three processes in order to determine which portion of the proton spin is carried by gluons. Better understanding of charmonium production at U70 energies is needed — for this aim, pion and proton beams will be used to produce charmonium. Gluon contribution into the proton spin as well as strange quarks and orbital momentum contributions are worldwide studies at HERMES, COMPASS, RHIC, JLAB and SLAC. Latest achievements issues in the determination of polarized parton distribution functions, driven by new measurements in polarized proton-proton collisions at the Relativistic Heavy Ion Collider, allowed to estimate [11] that the gluon contribution is positive in different approaches and equals  $\Delta G = 0.20^{+0.06}_{-0.07}$  for DSSV14 [12] and  $\Delta G = 0.23 \pm 0.06$  for NNPDFpol1.1. integrated in the interval  $x$  0.05 – 1 and  $Q^2 = 10 \text{ GeV}^2$  [13]. Nevertheless, these results are model dependent while SPASCHARM measurements will give unique possibility to measure  $\Delta G$  directly. Nevertheless, these results are model dependent while SPASCHARM measurements will give unique possibility to measure  $\Delta g$  directly. We propose a new experiment in this field — it should be complementary to the existing experiments. It will give new data at large  $x$  for global analysis. The biggest gluon polarization is anticipated near  $x = 0.3$ . SPASCHARM will measure gluon polarization in the region of  $x$  between 0.3 and 0.6.

Information about gluon polarization might be obtained through simultaneous measurements of  $A_{LL}$  in inclusive production of  $\chi_{c2}$  and  $J/\Psi$ . This experiment was proposed at Fermilab (P838) at 200 GeV as a continuation of E704 [14]. The Fermilab's PAC pointed out that physics was very interesting, but an intensity of the polarized proton beam from  $\Lambda$ -hyperon decays was small, so the statistics would not be enough. The experiment was not approved. .

The final goal of the proposed experiment is to measure double-spin asymmetry  $A_{LL}$  with the use of longitudinally polarized beam and target in the process:

$$p \rightarrow + p \rightarrow \rightarrow \chi_{c2}(J/\Psi) + X, (\chi_{c2} \rightarrow J/\Psi + \gamma).$$

$J/\Psi$  will be registered via  $\mu^+\mu^-$  decay due to Bremsstrahlung in  $e^+e^-$  decay mode. The charmonium states under study are  $J/\Psi(3096, J^{PC} = 1^{--})$ ,  $\chi_{c1}(3510, J^{PC} = 1^{++})$  and  $\chi_{c2}(3555, J^{PC} = 2^{++})$ . The measured experimental asymmetry is given by

$$A_{LL} = \frac{1}{P_B P_T^{eff}} \cdot \frac{I^{++} - I^{+-}}{I^{++} + I^{+-}} \quad (1)$$

where  $P_B$  is the beam polarization,  $P_T^{eff}$  is the effective target polarization,  $I^{++}$ ,  $I^{+-}$  are the number of events normalized to the incident beam intensity. The helicity  $(++)$  and  $(+-)$  states correspond to  $(\rightarrow\rightarrow)$  and  $(\leftarrow\rightarrow)$  states, respectively, where arrows indicate the beam and target spin direction in the laboratory system.

Theoretical predictions of  $A_{LL}$  mainly depend on two assumptions:

- gluon polarization  $\Delta G/G$  and
- charmonium production mechanism which defines  $A_{LL}$  at the parton level (in parton-parton interactions).

The experimental setup SPASCHARM is presented in Fig. 2. It is open geometry experiment. The main parts of the setup are as follows:

- wide aperture spectrometer with GEM, drift chambers and proportional chambers;
- electromagnetic calorimeter, and
- muon detector.

Fine segmented electromagnetic calorimeter of shashlik type with energy resolution  $\Delta E/E$  about 3% will be constructed. It is critically needed to detect very precisely  $\gamma$ -quanta from  $\chi$ -decays to separate  $\chi_{c1}$  and  $\chi_{c2}$  through high precision energy resolution of the calorimeter.

The principle point for this experiment is a separation of the two charmonium states with the spins equal to 1 and 2, namely  $\chi_{c1}(3510)$  and  $\chi_{c2}(3555)$ . The Monte-Carlo simulations for 45 GeV have been made. We can see that the two states of interest are well separated.

The SPASCHARM experiment plans to have 25000 electronic channels (7000 ADC, 2000 TDC and 16000 registers). The trigger for interaction in the target will be digitized in each sub-detector, pre-processed and buffered for further processing. A high level trigger selection will occur in compute nodes which access the buffers via a high bandwidth network fabric. The experiment plans to operate at interaction rates of the order of few hundred kHz (about 1 MHz for beam tracking). With pre-processing on the detector electronics for a substantial reduction of the data volume, typical event sizes are in the range of 2 to 4 kB. .

Our estimate has shown that we expect to get a precision of  $\sigma(A_{LL}) = 0.07$  for  $\chi_{c2}$  and 0.025 for  $J/\Psi$  at  $x = 0.3$  during 100 days of data taking.

With the use of polarized proton beam at SPASCHARM a precision measurement of single spin asymmetry in inclusive production of miscellaneous resonances in the transverse polarized beam fragmentation region in a wide  $(x_F, p_T)$ -region will be worthwhile. Also it will be possible to measure transversity in Drell-Yang muon (electron) pairs.

## 2.3 Polarized frozen-spin target at Protvino

The authors of the project suggest to use the modernized frozen-spin target based at the one, developed earlier at LNP JINR [15, 16].



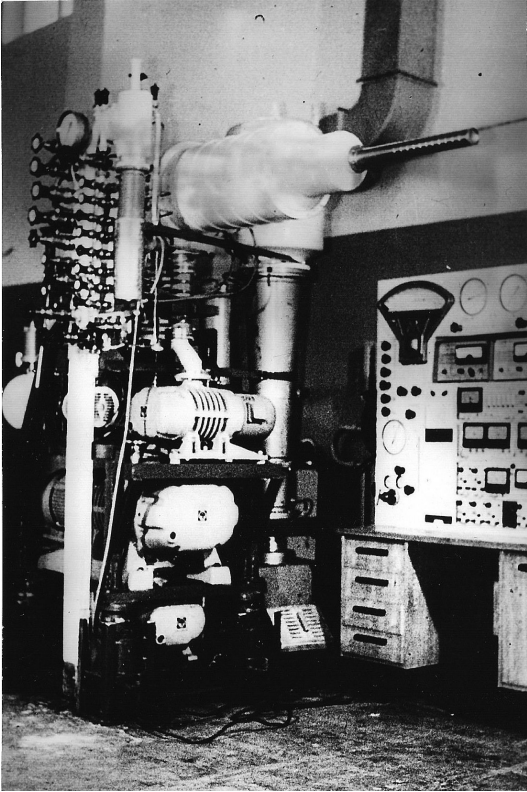


Figure 3: The frozen spin target before transportation from Dubna to IHEP (1978).

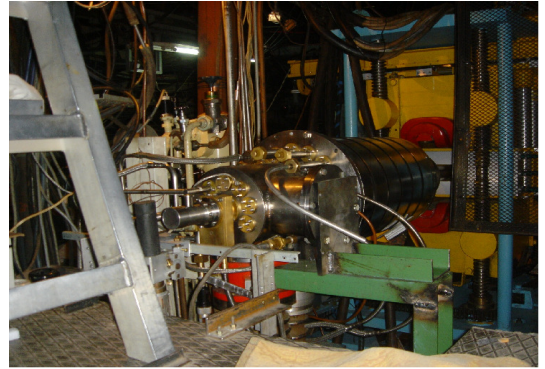


Figure 4: The frozen spin target at the beam area (Protvino).

The target includes a stationary cryostat with a dilution refrigerator, an electromagnet, a high-frequency generator providing the dynamic polarization and a NMR-signal detection array.

The main part of the apparatus is a horizontal cryostat of the  $^3\text{He}/^4\text{He}$  dilution refrigerator, which cools the target material during dynamic polarization and in the frozen mode (Figs. 3, 4). The "tail" of the cryostat is placed in the gap of a steel electromagnet with movable poles. In the DNP mode, the magnet poles are in the position when the magnetic circuit is closed, the magnetic field is as high as 2.5 T and the homogeneity is no worse than  $10^{-4}$  within the target volume. When the poles are open, the magnetic field is 0.4 T in a gap of 20 cm and the homogeneity is  $10^{-2}$ . This electromagnet was developed by IHEP experts.

Target material, 1,2-propanediol  $\text{C}_3\text{H}_8\text{O}_2$  (volume  $20\text{ cm}^3$ ) with a paramagnetic Cr(V) impurity, in the form of small balls  $\approx 2\text{ mm}$  in diameter, is placed in a teflon container, 2 cm in diameter and 6 cm long. The maximum obtained proton polarization was 93% and 98% for positive and negative values, respectively. In the DNP mode,  $T = 200\text{ mK}$ , the circulation rate of  $^3\text{He}$  is  $3 \times 10^{-2}\text{ mol/s}$ . An IMPATT diode generator with output power of  $\approx 200\text{ mW}$  at a frequency of  $\approx 70\text{ GHz}$  is used for the dynamic build-up of polarization. Polarization time necessary to obtain  $0.8P_{max}$  is  $\approx 40\text{ min}$ .

In the frozen spin mode the target is maintained at a temperature of 20 mK in the holding magnetic field of 0.45 T; the circulation rate of  $^3\text{He}$  is  $2 \times 10^{-3}\text{ mol/s}$ . Under these conditions, the

spin relaxation time was  $\approx 1200$  h for positive polarization and 800 h for negative polarization.

The target polarization measurement is carried out using a Q-meter of Liverpool type with operating frequency of about 106 MHz.

## 2.4 Main results

First data to study single-spin asymmetries in the SPASCHARM experiment were being taking in 2018 (analysis just started).

Publications: 1. The polarized proton and antiproton beam project at U-70 accelerator V.V. Abramov (Serpukhov, IHEP & Kurchatov Inst., Moscow) et al.. 2018. 7 pp. Published in Nucl. Instrum. Meth. **A 901** (2018) 62.

2. Measurements of the Beam and Target Analyzing Powers and Spin Correlation Parameter ANN in Elastic pp Scattering at 45 GeV/c. V.V. Abramov (Serpukhov, IHEP) et al.. 2018, Published in KnE Energ.Phys. **3** (2018) 326.

3. Comparative study of the inclusive asymmetries induced by polarized protons and antiprotons at 16 GeV/c at the U-70 accelerator V.A. Okorokov (Moscow Phys. Eng. Inst.) et al.. Oct 16, 2017. 7 pp. Published in J. Phys. Conf. Ser. **938** (2017) no.1, 012014.

4. Polarized proton and antiproton beams for the SPASCHARM experiment at U-70 accelerator I.I. Azhgirey et al, Published in J. Phys. Conf. Ser. **798** (2017) no.1, 012177.

5. Study of single-spin asymmetries with polarized target at the SPASCHARM experiment at U-70 accelerator V.V. Abramov (Serpukhov, IHEP) et al.. 2017. 5 pp. Published in J.Phys.Conf.Ser. 798 (2017) no.1, 012096.

6. Beam polarimetry at the SPASCHARM experiment at IHEP U-70 accelerator A.A. Bogdanov (Moscow Phys. Eng. Inst. & Kurchatov Inst., Moscow) et al.. 2017. 5 pp. Published in J. Phys. Conf. Ser. **798** (2017) no.1, 012179.

7. Simultaneous measurements of spin observables  $A_N$  and  $A_{NN}$  in elastic pp scattering (extension of the SPASCHARM program at U-70). V.V. Abramov (Serpukhov, IHEP) et al.. 2017, Published in J. Phys. Conf. Ser. **938** (2017) no.1, 012006.

## 3 GDH: Helicity dependence of single and double pion photoproduction processes and the GDH integral on the neutron

Traditionally, the main goal of meson photoproduction measurements is so named "complete" experiment, that allows to describe a reaction investigated in a model independent way.

A conception of the complete experiment in the two body scattering of particles with spin was firstly introduced by L.D. Puzikov, R.M. Ryndin and Ya.A. Smorodinsky in 1957.

Generally, there are 64 polarization observables for single and double pseudoscalar meson photoproduction. For double meson photoproduction we need to extract information on 8 helicity or transversity amplitudes. In this case, there are 28 relations and another 21 relations that arise from consideration of their phases, leaving 15 independent quantities [17]. For  $\gamma N \rightarrow \pi\pi N$  reaction, as an example, we must perform measurements for 8 independent observables

to obtain absolute magnitudes of the amplitudes plus 7 for independent phase differences. Moreover, it should be done at each kinematic point, which depends on 5 kinematic variables. It is practically impossible for today.

From this point of view, the single pseudoscalar meson photoproduction looks more realistic: we need to extract information on only 4 helicity or transversity amplitudes from 16 possible observables. Minimal "complete" set of experiments will require 7 measurements of carefully selected polarization observables in addition to the differential cross section at each kinematic point, which depends now only on 2 kinematic variables.

Experiments are conducted with the photon beam of the electron accelerator MAMI C, Mainz, Germany. Main experimental apparatus:

- 1) Tagged photon beam (unpolarized, circular polarization, linear polarization).
- 2) Detector system:

- $4\pi$  photon spectrometer CB/TAPS (100% solid angle covering for particles decaying into two or more secondary photons, 97% of  $4\pi$  for single photons, detection of neutrons and charged particles is also possible at restricted energy regions).

- Crystal Ball (CB) overlaps polar angle range  $(20 - 160)^\circ$  and TAPS:  $(1 - 20)^\circ$ . CB consists of 672 NaI(Tl) crystals with 15.7 radiation lengths.

- TAPS consists of 366 BaF<sub>2</sub> crystals with 12 radiation lengths and is supplemented by 5-mm plastic scintillator in front of each module (VETO).

- MWPC, 2 cylindrical multi-wire proportional chambers for vertex reconstruction, target position correction (z), and beam position control (x, y).

- PID (Particle Identification Detector) consists of a barrel of 24-mm-thick plastic scintillator strips. This is a VETO detector for photons in Crystal Ball, also it works as  $\Delta E/E$  detector for charged particles identification in Crystal Ball.

- Recoil proton polarimeter. Method: detection of proton scattered in the graphite analyzer and comparison its angle with kinematic reconstruction.

- 3) Dubna-Mainz Frozen Spin Target (available since 05.2010) uses Butanol or d-Butanol, <sup>3</sup>He/<sup>4</sup>He dilution refrigerator, superconducting holding magnet, with possible longitudinal and transverse polarizations.

- Maximal polarizations are; for protons -  $\simeq 90\%$ , for deuterons -  $\simeq 75\%$ .

- Maximal relaxation time is  $\simeq 2000$  hours.

- 4) New development: active (scintillating) polarized target.

### 3.1 Physics motivations

Experiment A2-9/05 to measure the helicity dependence of single and double photoproduction processes and the GDH integrand on the neutron has not requested beam time during the three years since it was approved with A-rating due to delays in the construction of the Mainz frozen spin (deuterated) butanol target. The goals of the proposal remain, however, as timely as ever. In the present proposal we aim to update the scientific case and broaden the experimental scope, using a recently developed high-pressure, longitudinally-polarized  $^3\text{He}$  target, which complements the properties of the frozen-spin target. The nucleus of a polarized  $^3\text{He}$  atom consists of two spin paired protons and a single unpaired neutron, making it appear approximately as a single polarized neutron. From calculations of the  $^3\text{He}$  nuclear wave function one expects that the unpaired neutron carries about 90% of the total  $^3\text{He}$  spin [18]. Hence, the absence of free neutron targets makes  $^3\text{He}$  a valuable tool in the polarization studies of the fundamental structure of the neutron. The combination of two different polarized "nuclear" neutron targets and the capability of the experimental apparatus to identify cleanly different partial reaction channels will allow a precise quantitative evaluation of the corrections due to the bound nature of the polarized neutrons thus permitting an accurate determination of both the GDH integrand on the free neutron spanning a wide energy range and of the  $\gamma n \rightarrow N\pi(\pi)$  channels.

The new solid-state polarized target suitable for an investigation of the spin structure of nucleons by doing double polarization experiments at the MAMI C accelerator was developed.

Some future experiments with this target are listed below:

- experimental verification of the Gerasimov-Drell-Hearn (GDH) sum rule in the energy range up to 1550 MeV;
- helicity dependence of  $\pi^0$ ,  $\pi^0\pi^0$ ,  $\pi^0\pi^+$  and  $\pi^+\pi^-$  production on the proton in the region of the  $D_{13}(1520)$  and  $F_{15}(1680)$  resonances (requires circularly polarized photons and longitudinally polarized protons);
- measurement of the  $G$  asymmetry in  $\gamma p \rightarrow p\pi^0$  and  $\gamma p \rightarrow n\pi^+$  (sensitive to the Roper resonance  $P_{11}(1440)$ ; requires linearly polarized photons and longitudinally polarized protons);
- photoproduction of  $\eta$ -mesons on the neutron: measurement of double polarization observable  $E$  (sensitive to  $D_{15}(1675)$  resonance; requires circularly polarized photons on longitudinally polarized deuterons);
- the total inclusive photoabsorption cross section on the deuteron in the photon energy range between 800 and 1550 MeV, where the statistical precision of the existing data is rather poor;

### 3.2 The GDH sum rule on the neutron

The Gerasimov-Drell-Hearn (GDH) sum rule [19, 20] relates the anomalous magnetic moment (AMM)  $\kappa$  of a particle of spin  $S$  and mass  $M$  to the integral over the weighted helicity

	p	n	d	${}^3\text{He}$
$\mu$	2.79	-1.92	0.86	-2.13
$\kappa$	1.79	-1.92	-0.14	-8.37
$I_{GDH}$	204	233	0.65	498

Table 1: The magnetic moment  $\mu$ , the AMM  $\kappa$  (in units of the nuclear magneton  $\mu_N$ ) and the GDH sum rule  $I_{GDH}$  in units of  $\mu\text{b}$  for protons, neutrons, deuterons and  ${}^3\text{He}$  nuclei.

asymmetry of the total absorption cross section for circularly polarized photons on a longitudinally polarized target:

$$I_{GDH} = \int_{\nu_{th}}^{\infty} \frac{\sigma_p - \sigma_a}{\nu} d\nu = 4\pi\kappa^2 \frac{e^2}{M^2} S, \quad (2)$$

where  $\nu$  is the photon energy and  $\sigma_p(\sigma_a)$  denote the total absorption cross sections for parallel (antiparallel) orientation of photon and particle spins. The inelastic threshold  $\nu_{th}$  corresponds to pion production (photodisintegration) threshold for a nucleonic (nuclear) target. This relation gives a fundamental connection between ground state properties of a particle and a moment of the entire excitation spectrum, showing the equivalence of a nonvanishing  $\kappa$  with the internal dynamical structure of the considered particle. A measurement of the GDH integrand then represents a fundamental test of our knowledge of photo-excitation of composite hadronic systems. Table 1 shows the magnetic moment ( $\mu$ ), the AMM and the GDH sum rule values for protons, neutrons, deuterons and  ${}^3\text{He}$  nuclei.

For the nucleon case, an estimate of the GDH sum rule value can be performed using a combination of multipole analyses of the available single pion photoproduction data (mostly from unpolarized experiments) [21, 22] and phenomenological models of multipion and heavy meson photoproduction reactions [23–25] up to  $E_\gamma \simeq 2$  GeV. Above this photon energy, the contribution can be estimated from Regge-type approaches [26].

In table 2 the current theoretical estimate of the GDH sum rule values is given for both the proton and the neutron. These estimates disagree with the expected GDH sum rule value for the proton while it roughly reproduces the neutron GDH value. However, the (proton-neutron) difference has a different sign with respect to the GDH expectation.

It is also instructive to perform the isospin decomposition of eq. 2 for the nucleon case, which results in:

$$I_{GDH}^{p,n} = \frac{2\pi^2 e^2}{m^2} (\kappa_s \pm \kappa_v)^2 = (I_{vv} + I_{ss} \pm I_{vs}), \quad (3)$$

where the subscripts  $s, v$  denote the isovector and isoscalar parts of the anomalous magnetic moment, respectively. The dominance of the isovector component ( $\kappa_v = 1.85\mu_N$ ) over the isoscalar one ( $\kappa_s = -0.06\mu_N$ ) is responsible of the extreme sensitivity of the isovector-isoscalar term  $I_{vs}$  in the GDH integral to the different models. This interference term is responsible for the ( $p - n$ ) difference of the sum rule. The first experimental check of the GDH sum rule for the proton was carried out jointly at the Mainz and Bonn tagged photon facilities, where  $I_{GDH}^p$  was measured in the photon energy range  $200 \text{ MeV} < E_\gamma < 2.9 \text{ GeV}$  [27–30]. The combination of this result with the theoretical predictions for the unmeasured energy ranges (see table 3 [31]) supports the validity of the GDH sum rule for the proton at odds with the estimates given in

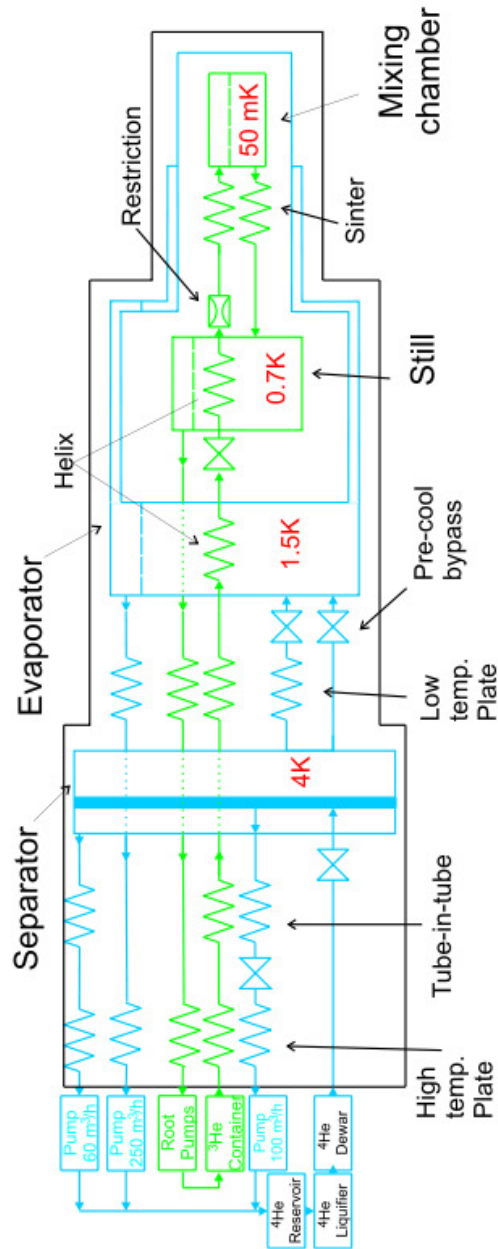


Figure 5: Schematic view of the Dubna-Mainz dilution cryostat.

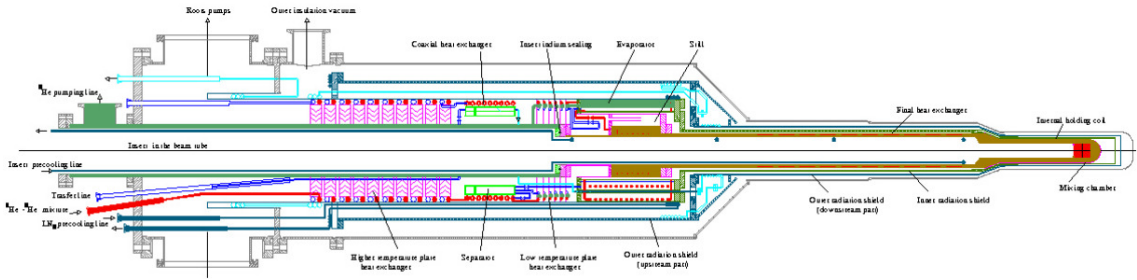


Figure 6: Schematic view of the Dubna/Mainz dilution refrigerator.

	$I_{GDH}$ proton	$I_{GDH}$ neutron
$\gamma N \rightarrow N\pi$	172[174]	147[131]
$\gamma N \rightarrow N\pi\pi$	94	82
$\gamma N \rightarrow N\eta$	-8	-6
$\gamma N \rightarrow K\Lambda(\Sigma)$	-4	2
$\gamma N \rightarrow N\rho(\omega)$	0	2
Regge contribution ( $E_\gamma > 2$ GeV)	-14	20
Total	$\approx 239$ [231]	$\approx 247$ [231]
GDH sum rule	204	233

Table 2: Contributions of different partial reaction channels to the GDH sum rule. Predictions for  $N\pi$  are from the SAID [21] and (within brackets) MAID [22] multipole analysis; estimates for  $N\pi\pi$  are from [23]; estimates for  $N\eta$  are from [22]; kaon channel contributions are from [24]; predictions for vector meson production are from [25]; Regge contributions are from [26].

table 2. The main reason of this discrepancy is the oscillating photon-energy dependence of the GDH integrand due to multipole contributions of alternating sign. Therefore, a reliable prediction requires a very high accuracy that has not been reached by any of the existing models.

This discrepancy emphasizes the need of a precise test of the GDH sum rule for both the neutron and proton and for precise double polarization data for all  $\gamma N \rightarrow N\pi(\pi)$  channels, which give the dominant contribution to the GDH integral, in order to pin down the origin of the existing discrepancies.

For the neutron, the interpretation of the experimental data is more complicated than in the proton case due to the lack of free neutron targets necessitating the use of neutrons bound in  $^2\text{H}$  or  $^3\text{He}$ . Nuclear structure effects and final state interactions prevent the direct access to the free neutron cross sections and theoretical support is needed for their evaluation. A quantitative extraction of  $I_{GDH}^n$  is then necessarily model dependent.

The combined use of both neutron-substitute targets and the capability of the experimental apparatus to separate different partial reaction channels will play a crucial role in constraining the theoretical analyses and in establishing the validity of the models that will be used for this extraction. In particular, the comparison between the two different "free neutron" values that are extracted from both the deuteron and  $^3\text{He}$  targets using different nuclear models will give

$E_\gamma$ (GeV)	$I_{GDH}^p$
$\leq 0.2$	$-28.5 \pm 2$
0.2 – 0.8 (measured)	$226 \pm 5 \pm 12$
0.8 – 2.9 (measured)	$27.5 \pm 2 \pm 1.2$
$\geq 2.9$	$-14 \pm 2$
Total	$211 \pm 5 \pm 12$
GDH sum rule	204

Table 3: The contribution (in  $\mu\text{b}$ ) of various energy regions to the GDH integral  $I_{GDH}^p$  on the proton. The contribution for  $E_\gamma < 0.2$  GeV is from the MAID [22] multipole analysis with an error estimated by a comparison with SAID [21]. The asymptotic contribution ( $E_\gamma > 2.9$  GeV) is from [26] with an error estimated by a comparison with a similar approach [32].

a fundamental cross-check of the reliability of the extraction procedures.

While in the deuteron the proton and the neutron are essentially in s states of relative motion with aligned spins,  $^3\text{He}$  is a system of two protons with spins paired off and an "active" unpaired neutron, again in relative s states. As a result we then find (see table 1) that

$$\mu_d \approx \mu_p + \mu_n; \quad \mu_{^3\text{He}} \approx \mu_n,$$

so that the  $^3\text{He}$  spin structure function is much closer to the free neutron than the deuteron. Therefore, it is expected that the measured GDH integrand function for  $^3\text{He}$  above the pion photoproduction threshold will already be a good first approximation of the  $I_{GDH}^n$  value. A more quantitative evaluation can be performed by considering the part of the GDH integral for deuteron and  $^3\text{He}$  above the pion production threshold.

### 3.3 Helicity dependence of meson photoproduction on the proton

We propose to perform a precise measurement of the helicity asymmetry of meson photoproduction with neutral final states using the Crystal Ball/TAPS setup together with the new Mainz frozen-spin target and the circularly polarized photon beam at MAMI C. Single  $\pi^0$  production reveals a strong sensitivity to the  $D_{13}(1520)$ - and  $F_{15}(1680)$  resonances,  $\eta$  production will allow to investigate the contribution of  $P_{11}(1710)$ ,  $S_{11}(1650)$ , and  $F_{15}(1680)$  resonances. The helicity asymmetry and helicity dependent invariant mass distributions in double  $\pi^0$ ,  $\pi^+\pi^0$  and  $\eta\pi^0$  production will help to pin down resonance contributions in the intermediate states and to clarify the dominant reaction mechanisms. The contribution of these reaction channels to the GDH integrand will be determined. Recently first preliminary results from the "Crystal Barrel at ELSA" and the "CLAS collaboration at JLAB" have been shown on the NSTAR 2009 conference. However, these data sets start at a photon energy above 500 MeV. On the other hand there have been shown preliminary data from the "LEGS experiment at BNL Brookhaven" in the  $P_{33}(1232)$  resonance region that show a discrepancy with the old data acquired with the DAPHNE detector in Mainz. The new experiment in Mainz with the Crystal Ball/TAPS setup specialized on multiphoton final states together with the new Mainz frozen-spin target will deliver a data set with high systematic and statistical accuracy in the MAMI





Figure 7: The new dilution refrigerator for the Crystal Ball frozen spin target.

C energy range from threshold up to 1400 MeV and in addition link together and crosscheck results from other laboratories.

The experiment will be performed at the tagged photon facility of MAMI (Glasgow-Tagger). Circularly polarized photons will be used in combination with a longitudinally polarized target and the  $4\pi$  Crystal Ball photon spectrometer with TAPS as forward wall and a Cherenkov detector for suppression of electromagnetic background.

### 3.4 Measurement of the $G$ asymmetry in $\vec{\gamma}\vec{p} \rightarrow p\pi^0$ and $\vec{\gamma}\vec{p} \rightarrow n\pi^+$

We propose to perform a precise measurement of the  $G$  observable in  $\vec{\gamma}\vec{p} \rightarrow p\pi^0$  and  $\vec{\gamma}\vec{p} \rightarrow n\pi^+$  in the tagged photon energy region of 250-800 MeV in order to determine the  $M_{1-}$  partial wave, which is sensitive to the Roper resonance  $P_{11}(1440)$ . Measuring both single pion channels will allow an isospin separation ( $M_{1-}$  for  $I = 1/2$  and  $I = 3/2$ ). Recently first preliminary results for the observable  $G$  from the "CBELSA/TAPS collaboration" and "CLAS collaboration" have been shown at the NSTAR 2009 conference. However these preliminary data sets start at a photon energy above 500 MeV.

We require a beam of linearly polarized photons on a longitudinally polarized butanol target and the  $4\pi$  Crystal Ball photon spectrometer in combination with TAPS as forward wall, the DAPHNE tracker and a scintillator PID. The new tagging system will provide the intense, linearly polarized photon beam.

### 3.5 Transverse asymmetries $T$ and $F$ in $\eta$ photoproduction in the $S_{11}(1535)$ region

We propose to measure the target asymmetry  $T$  and the double-polarization observable  $F$  for  $\eta$  photoproduction in order to investigate interference effects between the  $S_{11}(1535)$  and the  $D_{13}(1520)$  nucleon resonances and to determine the energy-dependent phase shift between  $s$  and  $d$  waves, which is not yet taken into account by isobar models (MAID, SAID) for  $\eta$  photoproduction.

We require a beam of circularly polarized photons, energy-tagged by the new tagging system, in combination with a transversely polarized frozen-spin butanol target. The reaction products will be detected using the Crystal Ball/TAPS  $4\pi$  photon spectrometer; the PID detector and the cylindrical MWPC will perform particle identification and track reconstruction for charged particles.

### 3.6 Spin observables for $\pi\eta$ photoproduction in the $D_{33}(1700)$ region

Recently measured total and differential cross sections for the reaction  $\gamma p \rightarrow \pi^0 \eta p$  indicate a dominance of the  $\Delta(1700)D_{33}$  resonance in the energy range  $E_\gamma = 0.95 - 1.4$  GeV. We propose to make use of this dominance to study systematically properties of the  $D_{33}(1700)$  as well as other partial wave amplitudes that reveal themselves via interference with it. Such bilinear combinations of partial wave amplitudes can be extracted by measuring the transverse spin observables  $T$  and  $F$ .

The experiment will be performed at the new tagged photon facility of MAMI using the Crystal Ball/TAPS detector setup together with a transversely polarized frozen-spin butanol target and circularly polarized photon beam.

### 3.7 Measurement of polarized target and beam asymmetries in pion photo-production on the proton: test of chiral dynamics

We propose to perform precise measurements of the  $\vec{\gamma}\vec{p} \rightarrow p\pi^0$  reaction from threshold to partway up the  $\Delta$  resonance using polarized beams and targets. These measurements will provide an additional, stringent test of our current understanding that the pion is a Nambu-Goldstone boson due to the spontaneous chiral symmetry breaking in QCD. Specifically we will test detailed predictions of chiral perturbation theory (ChPT) and its energy region of convergence. This experiment will test strong isospin breaking due to the mass difference of the up and down quarks. The data on the (time reversal odd)transversely polarized target asymmetry  $T = A(y)$  will be sensitive to the  $\pi N$  phase shifts and will provide information for neutral and charge states ( $\pi^0 p$ ,  $\pi^+ n$ ) in a region of energies that are not accessible to conventional  $\pi N$  scattering experiments. The data on the double polarization observable  $F = A(\gamma_c, x)$  (circularly polarized photons-transversely polarized target) will be sensitive to the  $d$ -wave multipoles, which have recently been shown to be important in the near threshold region.

We require a beam of tagged, circularly polarized photons incident on a transversely polarized butanol target. The detector will consist of the Crystal Ball photon spectrometer in combination with TAPS as forward wall. The new tagging system and the polarized electrons will be utilized.

### 3.8 Measurement of the proton spin polarizabilities

We propose to perform three precise Compton scattering experiments to extract the spin polarizabilities of the proton. These four structure constants are fundamental observables describing the spin response of the nucleon, and they have generated considerable theoretical interest in recent years. Using subtracted dispersion relations, the values of the known static polarizabilities,  $\alpha_{E1}$  and  $\beta_{M1}$ , and a measurement of one beam and two beam-target asymmetries, we intend to extract all four quantities. The experiment will be performed at the new

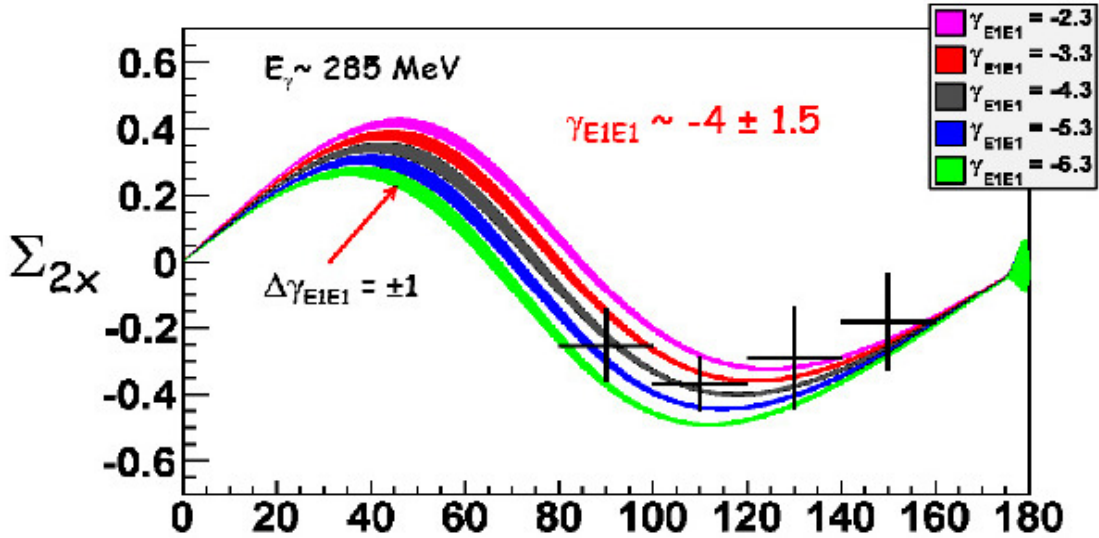


Figure 8: Proton spin polarizability  $\gamma_{E1E1}$  obtained from the measurement of the Compton scattering asymmetry  $\Sigma_{2x}$ . The points are the experimental data, the curves are dispersion model calculations. The horizontal axis indicates the scattering angle.

tagged photon facility of MAMI using polarized photon beams (both linear and circular) on both polarized (butanol) and unpolarized (liquid hydrogen) targets, with the reaction products being detected using the CB/TAPS system.

### 3.9 Photoproduction of pions off polarized neutrons

The focus of this proposal is the production of pions and the study of their interactions with transversely and longitudinally polarized neutrons. Our program centers on the use of real polarized photons to produce short-lived mesons on polarized and unpolarized nucleon targets. With the recent upgrade of MAMI-C to 1.6 GeV, we can now produce the complete nonet of pseudoscalar mesons. The results of our program will be used to test theoretical predictions based on QCD, lattice QCD, and different dynamical models. They will also be used to expand the GW SAID, BnGa, JuBo, and MAID analyses in an energy region from the pion threshold to 1.6 GeV. These data will also provide coherent  $\pi^0$  production off the polarized deuteron which will allow us to expand our studies of the reaction mechanism of this process.

The experiment will be performed using the  $4\pi$  Crystal Ball (CB) spectrometer in conjunction with the TAPS detector at MAMI. The facilities at MAMI needed for this proposal

include tagged, linearly polarized photons provided by the new Tagger and transversely and longitudinally polarized (deuterated) targets [33, 34].

### 3.10 Polarized frozen-spin target at Mainz

Polarization experiments using high density solid-state targets in combination with tagged photon beams can reach the highest luminosities. For the double polarization measurements planned with the Crystal Ball detector on polarized protons and deuterons a specially designed, large horizontal  $^3\text{He}/^4\text{He}$  dilution refrigerator has been built in cooperation with the Joint Institute for Nuclear Research. It has minimum limitations for the particle detection and fits into the central core of the inner Particle Identification Detector (PID2). This was achieved by using the frozen spin technique with the new concept of placing a thin superconducting holding coil inside the polarization refrigerator. Longitudinal and transverse polarizations are possible. Highest nucleon polarization in solid-state target materials is obtained by a microwave pumping process, known as "Dynamic Nucleon Polarization" (DNP). This process is applicable to any nucleus with spin and has already been used in different experiments with polarized proton and deuteron targets. The geometric configuration of the target is the same for the polarized proton and deuteron setup. However, since the polarization measurement of the deuteron is more delicate due to the small value of the polarization signals, the modification of some basic components is needed. The reason for this is twofold: firstly the magnetic moment of the deuteron is smaller than that of the proton and, in addition, the interaction of the deuteron quadrupole moment with the electric field gradient in the sample broadens the deuteron polarization signal. An accuracy  $\delta P_p/P_p$  of 2 to 3% for the protons and  $\delta P_d/P_d$  of 4 to 5% for the deuterons is expected in the polarization measurement. It has also to be taken into account that the measured deuteron polarization  $P_d$  is not equal to the neutron polarization  $P_n$ . Assuming a 6% admixture of the D-state of the deuteron, a calculation based on the Clebsch-Gordon coefficients leads to  $P_n = 0.91P_d$ . Several polarized proton and deuteron materials are available such as alcohols and deuterated alcohols (e.g. butanol  $\text{C}_4\text{H}_9\text{OH}$ ),  $\text{NH}_3$ ,  $\text{ND}_3$  or  $^6\text{LiD}$ . The most important criteria in the choice of material suitable for particle physics experiments are the degree of polarization  $P$  and the ratio  $k$  of free polarizable nucleons to the total number of nucleons. Further requirements on polarized target materials are a short polarization build-up time and a simple, reproducible target preparation. The polarization resistance against radiation damage is not an issue for experiments with a low intensity tagged photon beam ( $\dot{N}_\gamma \approx 5 \times 10^7 \text{ s}^{-1}$ ) as will be used here. However, the limitations of a reduced relaxation time due to overheating of the target beads (Kapitza resistance) will have to be investigated.

Taking all properties together, butanol and deuterated butanol are the best material for this experiment. For protons we have a maximum polarization of  $P_p = 90\%$  and an average polarization of  $P_p = 70\%$  in the frozen spin mode. Recently, a deuteron polarization  $P_d = 80\%$  was obtained with Trityl doped butanol targets at 2.5 T magnetic field in a  $^3\text{He}/^4\text{He}$  dilution refrigerator. At a 0.5 T holding field an average neutron polarization  $P_n$  of 50% was obtained. The filling factor for the  $\sim 2$  mm diameter butanol spheres into the 2 cm long, 2 cm diameter target container equals around 60%. At a total tagged photon flux of  $5 \times 10^7$  and a target temperature 30 mK relaxation times of about 2000 hours was obtained [35]. The polarization has to be refreshed by microwave pumping approximately once a week of experiment running

time. In conclusion, main target parameters are presented:

- Maximum total tagged photon flux in the energy range of 4.7 to 93% of  $E_0$ :  $\dot{N}_\gamma \approx 5 \cdot 10^7$  s<sup>-1</sup>, with relaxation time of 2000 hours.
- Target proton density in 2 cm cell:  $N_T \approx 9.1 \cdot 10^{22}$  cm<sup>-2</sup> (including dilution and filling factors).
  - Average proton polarization  $P_p = 70\%$ .
- Target deuteron density in 2 cm cell:  $N_T \approx 9.4 \cdot 10^{22}$  cm<sup>-2</sup> (including dilution and filling factors).
  - Average neutron polarization  $P_n = 50\%$ .

The new Mainz frozen spin target will be used together with the Crystal Ball detector in order to perform double polarization experiments, that will bring new information about the spin structure of the nucleons. As it was shown earlier, to polarize a target material high magnetic fields and low temperatures are required. Temperatures in the mK range are achieved with a dilution refrigerator. It should fit in the geometry of the Crystal Ball detector, therefore has to be horizontal and with a well defined maximum radius. A superconducting magnet provides a magnetic field of up to 5 T with high homogeneity. A microwave system enlarges the degree of polarization via the dynamical nuclear polarization (DNP) method. The developed nuclear magnetic resonance (NMR) system will provide an accurate measurement of the degree of polarization. The next sections will present the main parts of the Mainz frozen spin target, and its actual status.

### 3.10.1 Refrigerator

The horizontal dilution cryostat has been developed in close collaboration with the polarized target group of the Joint Institute for Nuclear Research, Dubna, ([36–39, 74]). Fig. 5 shows a schematic view of the cryostat. The <sup>4</sup>He pre-cooling system is pictured in blue, and the <sup>3</sup>He line in green color. The outgoing helium gas is collected in a reservoir container and afterwards liquified in a standard Linde liquifier. <sup>4</sup>He is inserted from a Dewar into the *separator*. A needle valve controls this flow. In this vessel the helium is separated into gas and liquid phases. A superconducting wire is used to measure the level of liquid helium. One 60 m<sup>3</sup>/h rotary pump circulates the gas through different heat exchangers attached to the external shield to thermally isolate the inner part of the cryostat. Another 100 m<sup>3</sup>/h rotary pump reduces the vapor pressure from above the liquid, cooling down the separator. This outgoing gas pre-cools the incoming <sup>3</sup>He gas in two steps with some high temperature and tube-in-tube heat exchangers (HE). One needle valve manages the outgoing flow between the two HEs.

Liquid helium from the separator can move to the *evaporator* pot via a HE, where the incoming <sup>3</sup>He is liquified, or directly through a bypass for the cool down process, since the flow resistance of the HE is too high for warm gas. Two needle valves rule these possibilities. As in the separator, the level of liquid is measured with a superconducting wire. The temperature in the evaporator is reduced down to about 1.5 K by exhausting helium with a 250 m<sup>3</sup>/h rotary

pump. This gas is also used to cool down the incoming gas. The evaporator surrounds the *still* vessel and thermally isolates it.

The incoming  $^3\text{He}$  liquid passes through an helix immersed in the cold helium of the evaporator and another one inside the still. Behind the still are ten sintered heat exchangers that reduce the temperature of the liquid  $^3\text{He}$  as much as possible before it enters the *mixing chamber*. There the diluted-concentrated phase separation is produced and the lowest temperatures are achieved. Liquid from the diluted phase goes to the still via the sintered heat exchangers pre-cooling the incoming  $^3\text{He}$ .

A heater is placed in the still to evaporate the liquid. This gas is pumped out by powerful roots pumps, and in its way out it cools the whole cryostat. After the roots pumps the warm gas is re-injected and the continuous process starts again.

### 3.10.2 Polarizing magnet

In order to polarize the target material a superconducting magnet able to produce up to 5 Tesla with a central homogeneity of  $\Delta B/B \leq 10^{-4}$  is used. The high compact field solenoid consists of a single block of multifilamentary NbTi wound onto an stainless steel former. The conductor is casted in epoxy resin to eliminate wire movement. The inductance of the coil is 17.5 H. It is immersed in a bath of liquid  $^4\text{He}$ . Radiation heat load is minimized by the use of high purity aluminium nitrogen-cooled radiation shield, and multi-layer superinsulation enclosed in vacuum.

The magnet contains a 70 liter nitrogen storage dewar, and a 100 liter liquid helium reservoir monitored with a helium level meter HLG200/210 with a probe type 250 from Cryogenic Limited. Three RhFe thermometers, with a well defined response between 300 and 4.2 K, attached to the superconducting coil, the helium reservoir and the insulation respectively provide an immediate indication of temperatures from four terminal resistance measurements.

The magnet control system was developed mainly by the company Cryogenic Limited. The power supply able to produce the 97.06 A needed to achieve 5 T incorporates a sophisticated microprocessor unit, with all operations monitored through the internal firmware. It is connected to a PC via an IEEE-488 interface, and it is fully controlled by a LabView program. The ramping speed and maximum current can be set, and the induced magnetic field is continuously displayed. The temperature sensors and the helium level gauge are verified at any time by the program.

A superconducting persistent mode switch is connected in parallel to the magnet coil and wired to the main input/output current terminals. Resistive heaters wound into the switch enable it to be either resistive or superconducting.

The outer magnetic field was simulated and successfully compared with measurements. Just 20 cm away from the center of the coil less than 10 Gauss are measured, therefore, no electromagnetic devices will be affected by it.

About 100 liters of liquid nitrogen are initially needed to cool the shielding. It takes around 10 hours to cool it down from room temperature to 100 K. After 3 days the rest of the magnet is below 200 K. The  $^4\text{He}$  reservoir and the solenoid container are then pre-cooled by a small amount of liquid nitrogen within 1 hour. With the system pre-cooled and all nitrogen expelled, liquid helium can be transferred into the dewar via the siphon port. In about 3 hours the magnet coil reaches temperatures of 4.2 K and the reservoir container starts to fill. It is also

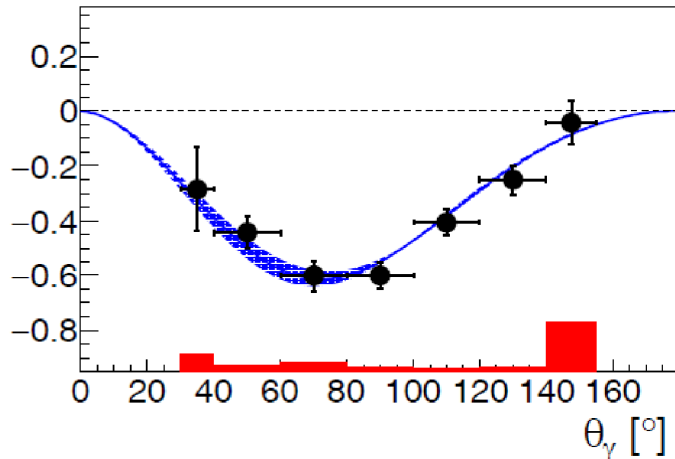


Figure 9: Beam asymmetry  $\Sigma_3$  in the range 119-139 MeV. Points – experiment, the curve – ChPT calculation (publication [1]).

possible to pre-cool the magnet using only the liquid nitrogen shielding container. This method avoids the complicated process of extracting the nitrogen from the helium pot. If the nitrogen container is filled for at least 7 days temperatures below 150 K are achieved in the magnet can and in the helium reservoir. The helium consumption of the magnet is less than 1 m<sup>3</sup>/h gas in stable operation, and about 1.5 m<sup>3</sup>/h when it is operated at magnetic fields of 2.5 T.

The magnet was manufactured by Cryogenic Limited and delivered in 2002.

### 3.11 Main results

1. The first ever successful experiment with the active polarized target has been realized at the beam of circularly polarized tagged photons of the MAMI accelerator (Mainz). High efficiency and low threshold for the detection of the recoil protons in the target open new perspectives for the study of the proton spin structure and extraction of the model-independent data. Polarization observables for  $\pi^0$  and  $\pi^+$  photoproduction has been measured, as well as Compton scattering asymmetries allowing to extract model-independent data on the proton spin polarizabilities.

2. First ever measurements of the beam asymmetry  $\Sigma_3$  for Compton scattering below pion photoproduction threshold have been performed (Fig. 9) by A2 collaboration at the polarized energy marked photon beam of the MAMI accelerator (Mainz). The results confirm the existing predictions of perturbation theory and dispersion relation models and deviate notably from the Born term in which the contributions of the proton polarizabilities are not included. The results obtained show that the extraction of the scalar polarizabilities from the beam asymmetry below the threshold provides an alternative to the extraction from the unpolarized Compton scattering cross section (publication [1]).

3. The reactions  $\gamma p \rightarrow \eta p$  and  $\gamma p \rightarrow \eta' p$  have been measured from their thresholds up to the center-of-mass energy  $W = 1.96$  GeV with the tagged-photon facility at the Mainz microtron MAMI. Differential cross sections were obtained with unprecedented accuracy, providing fine energy binning and full production-angle coverage. A strong cusp is observed in the total  $\eta$  photoproduction cross section at the energies in vicinity of the  $\eta'$  threshold,  $W = 1896$  MeV



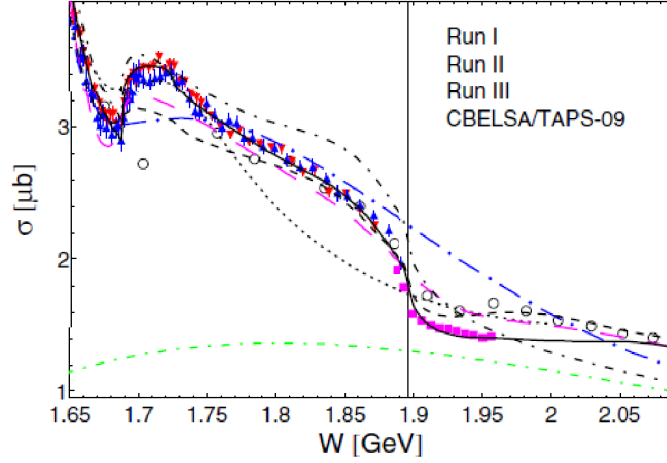


Figure 10:  $\gamma p \rightarrow \eta p$  total cross section.

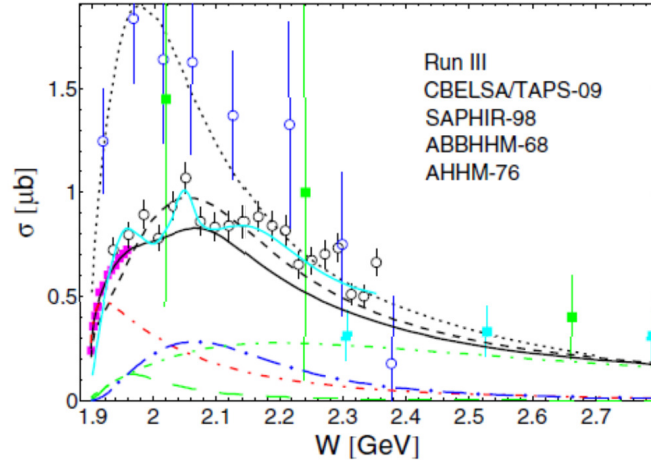


Figure 11:  $\gamma p \rightarrow \eta' p$  total cross section.

( $E_\gamma = 1447$  MeV) (Fig. 10). This behavior in combination with the steep rise of the total  $\eta'$  - photoproduction cross section from its threshold (Fig. 11) is explained in a revised  $\eta$ MAID2017 isobar model by a contribution of the  $N(1895)1/2^-$  nucleon resonance. The new precision data allowed to determine properties of this resonance (publication [2]).

4. The decay  $\eta \rightarrow 3\pi$ , which is forbidden by isospin symmetry, mostly occurs due to the difference in the mass of the u and d quarks. A precision measurement of this decay for both charged and neutral modes can be used as a sensitive test for the magnitude of isospin breaking in QCD. The A2 collaboration has measured the reaction  $\gamma p \rightarrow \eta p$  with high statistics at the MAMI accelerator. Most precise, at the moment, data on the  $\eta \rightarrow 3\pi^0$  decay were obtained from these measurements, which allowed the detailed study of its dynamics. The present data are compared to recent theoretical calculations (Fig. 12) (publication [3]).

PUBLICATIONS:



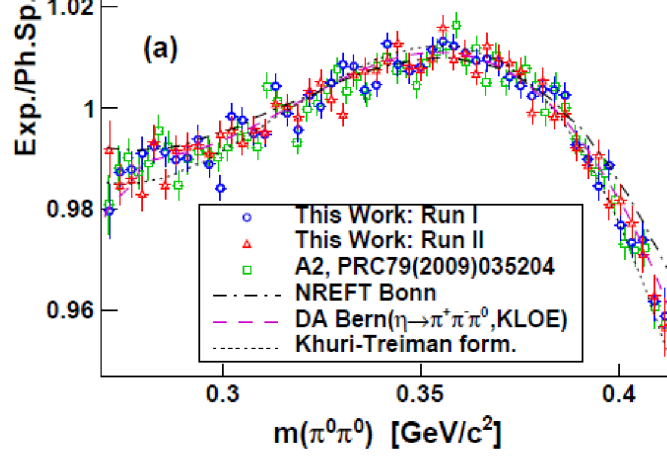


Figure 12: Explanation in the text.

1. V. Sokhoyan, N.S. Borisov, G.M. Gurevich, A.B. Lazarev, A.B. Neganov, Yu.A. Usov et al. Determination of the scalar polarizabilities of the proton using beam asymmetry  $E_3$  in Compton scattering. *Eur. Phys. J. A* **53** No. 2 (2017) 14.

2. V. L. Kashevarov, N.S. Borisov, G.M. Gurevich, A.B. Lazarev, A.B. Neganov, Yu.A. Usov et al. Study of 7 and 70 photoproduction at MAMI. *Phys. Rev. Lett.* **118** No. 21 (2017) 212001.

3. P. Adlarson et al. Measurement of the  $\omega \rightarrow \pi^0 e^+ e^-$  and  $\eta \rightarrow e^+ e^- \gamma$  Dalitz decays with the A2 setup at MAMI. *Phys. Rev. C* **95** (2017) 035208.

4. P. Adlarson et al. Measurement of the  $\pi^0 \rightarrow e^+ e^- \gamma$  Dalitz decay at the Mainz Microtron. *Phys. Rev. C* **95** (2017) 025202.

5. L. Witthauer et al. Helicity-dependent cross sections and double-polarization observable  $E_3$  in  $\eta$  photoproduction from quasifree protons and neutrons. *Phys. Rev. C* **95** (2017) 055201.

6. M. Dieterle et al. First measurement of the polarization observable  $E_3$  and helicity-dependent cross sections in single  $\pi^0$  photoproduction from quasi-free nucleons. *Phys. Lett. B* **770** (2017) 523.

7. S. Prakhov, N.S. Borisov, G.M. Gurevich, A.B. Lazarev, A.B. Neganov, Yu.A. Usov et al. High-statistics measurement of the  $\eta \rightarrow 3\pi^0$  decay at the Mainz Microtron. *Phys. Rev. C* **97** No. 6 (2018) 065203.

8. P. Adlarson et al. Measurement of the decay  $\eta' \rightarrow \pi^0 \pi^0 \eta$  at MAMI. *Phys. Rev. D* **98** (2018) 012001.

9. M. Dieterle et al. Photoproduction of  $\pi^0$  Mesons off Protons and Neutrons in the Second and Third Nucleon Resonance Region. *Phys. Rev. C* **97** (2018) 065205.

10. A. Kaeser et al. First measurement of helicity-dependent cross sections in  $\pi^0 \eta$  photoproduction from quasi-free nucleons. *Phys. Lett. B* **786** (2018) 305.

11. C. S. Akondi et al. Experimental study of the  $\gamma p \rightarrow K_0 \Sigma^+$ ,  $\gamma n \rightarrow K_0 \Lambda$ , and  $\gamma n \rightarrow K_0 \Sigma_0$  reactions at the Mainz Microtron. *Eur. Phys. J. A* **55** (2019) 11, 202.

12. M. Bashkanov et al. Deuteron photodisintegration by polarized photons in the region of the  $d^*(2380)$ . *Phys. Lett. B* **789** (2019) 7.

13. W. J. Briscoe et al. Cross section for  $\gamma n \rightarrow \pi_0 n$  at the Mainz A2 experiment. *Phys.*

Rev. **C 100** (2019) 6, 065205.

14. V. Sokhoyan et al. Measurement of the beam-helicity asymmetry in photoproduction of  $\pi_0\eta$  pairs on carbon, aluminum, and lead. Phys. Lett. **B 802** (2020) 135243.

15. M. Bashkanov et al. Signatures of the  $d^*(2380)$  Hexaquark in  $d(\gamma, pn)$ . Phys. Rev. Lett. **124** (2020) 13, 132001.

16. D. Paudal et al. Extracting the spin polarizabilities of the proton by measurement of Compton double-polarization observables. Phys. Rev. **C 102** (2020) 3, 035205.

17. M. Dieterle et al. Helicity-Dependent Cross Sections for the Photoproduction of  $\pi_0$  Pairs from Nucleons. Phys. Rev. Lett. **125** (2020) 6, 062001.

18. C. Mullen et al., Single  $\pi_0$  production off neutrons bound in deuteron with linearly polarized photons. Eur. Phys. J. **A 57** (2021) 6, 205.

19. E. Mornacchi et al., Measurement of Compton Scattering at MAMI for the Extraction of the Electric and Magnetic Polarizabilities of the Proton. Phys. Rev. Lett. **128** (2022) 13, 132503.

### 3.12 CBELSA-Bonn

Besides Mainz, the frozen spin target is used at the Electron Stretcher Accelerator (ELSA) located in Bonn. It provides a beam of polarized electrons with energy up to 3.2 GeV. Physical motivation for experiments in Bonn in principle the same as for A2 at MAMI Collaboration. But more higher beam energy allows to search for missing baryon resonances. In Fig. 13 are schematically shown spectra of the nucleon (a) and delta (b) resonances as a dependence of mass (vertical axis). The most of missing resonances are above of  $M > 2.2$  GeV, that is higher of possible energy region of the MAMI accelerator.

At accelerator ELSA in Bonn, a linearly polarised photon beam was produced from the incident 3.2 GeV electron beam via coherent bremsstrahlung off a carefully aligned diamond crystal. For a coherent edge at  $E_\gamma = 950$  MeV a maximum polarisation of 65 % was reached. A circularly polarised photon beam was produced from a longitudinally polarised 2.4 GeV electron beam provided by ELSA. The polarisation was measured with a Moller polarimeter, a maximum electron polarisation of 64 % was reached. The electrons, after hitting the radiator target, passed through a magnet onto a tagging hodoscope which defined the energy of the bremsstrahlung photons. At the last experiments is used the MAINZ-DUBNA frozen spin butanol target. The detector system consisted of two electromagnetic calorimeters, the Crystal Barrel and the MiniTAPS detector, together covering the polar angle range from  $1^\circ$  to  $156^\circ$  and the full azimuthal angle. For charged particle identification, a three-layer scintillating fibre detector surrounding the target, and plastic scintillators in forward direction

could be used. The detector setup provided a high detection efficiency for photons and is therefore ideally suited to measure single and double polarisation observables in reactions with neutral mesons decaying into photons in the final state. Schematic view of the CBELSA experimental setup is presented in Fig. 14.

Program of both experiments (A2-Mainz and CBELSA-Bonn) is directed at the study of various aspects of the QCD spin-flavor structure of the nucleons. It includes the verification of Gerasimov-Drell-Hearn (GDH) sum rule for proton and neutron in a wider energy range. Precise measurements of the helicity asymmetry of meson photoproduction with different final states (including neutral ones) will give more detailed information on nucleon resonance properties

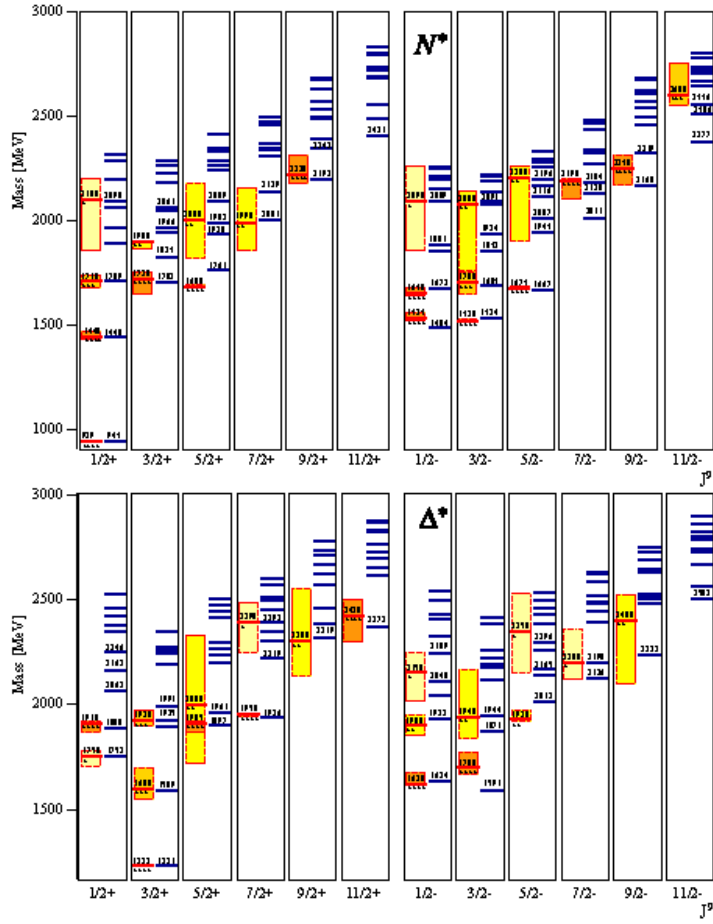


Figure 13: Blue lines depict the predicted nucleon resonances with  $I = 1/2$  (top) and delta resonances with  $I = 3/2$  (bottom) of the Bonn model. Each state is characterized by the total angular momentum  $J$  and parity  $P$  (+ -). The experimentally observed states are given by red lines and the yellow and orange boxes indicate their measurement uncertainties.

and multipole amplitudes.

Measurements using different combinations of beam and target polarizations will allow the determination of polarization observables with high quality. An extraction of the spin polarizabilities of nucleons from experimental data is also envisaged.

The multipole analysis of the obtained experimental data with the help of the gradually improving MAID package [2] provides a firm basis for a theoretical treatment. The last modification of the package [3] is already available on-line: <https://maid.kph.uni-mainz.de/eta2018/etamaid2018.html>. Presently there is also an intense theoretical activity to improve and optimize various calculational schemes including the Lattice QCD and the Chiral Perturbation Theory.

During 2018-2021 Dubna-Mainz polarized target was used by the CBELSA Collaboration in Bonn. Experimental data obtained in this experiment now are analyzed. Preliminary results were presented at PANIC2021 Conference [1]. Now new Dubna-Bonn cryostat for the frozen spin polarized target was designed and manufactured in JINR for the CBELSA Collaboration and it was successfully delivered from Dubna to Bonn.

1. F. Afzal for the CBELSA/TAPS Collaboration. Results of polarization observables in photoproduction reactions from the CBELSA experiment. PANIC2021 Conference, Lisbon Portugal. 5 - 10 September 2021. Book of Abstracts, p. 143. <https://indico.lip.pt/event/592/book-of-abstracts.pdf>

### 3.13 P2MESA-Mainz

MESA (Mainz Energy-recovering Superconducting Accelerator) is a new electron accelerator in Mainz. It will be able to generate a beam of extremely high intensity (150  $\mu$  A beam of alternately polarized electrons) that would otherwise require massive amounts of power so that a great number of particles can be focused on a tiny area of the target. It will thus be possible to produce a correspondingly high rate of particle collisions within a short period of time. The quality of the beam produced by MESA will be second to none, all electrons will be provided with the exact same kinetic energy of 155 MeV in the accelerator. These are optimal conditions for important precision experiments.

So, MESA will offer ideal conditions to explore the limits of the Standard Model. The Standard Model provides explanations for many of the natural processes that occur in the universe, however, there is a multitude of questions that still remain to be answered. Precision experiments at the MESA accelerator play a crucial role answering these questions. Several key experiments are currently under development, one of them, P2 (see Fig. 15).

The P2 experiment aims for a high precision measurement of an important natural constant: the mixing angle of the electroweak interaction (weak mixing angle). It is one of the quantities that are not predicted in the Standard Model, but predictions of the Standard Model depends on this value.

The weak mixing angle have to be determined experimentally. The cosine of this angle appears as the quotient of the masses of the W and Z bosons. This angle determines also the structure of neutral currents and the relationship between the constants g and e of the weak and electromagnetic interactions, respectively. The weak mixing angle cannot be measured directly, but can be indirectly determined in various ways. The independent measurement of this angle is an important test of precision for the validity of the Standard Model.

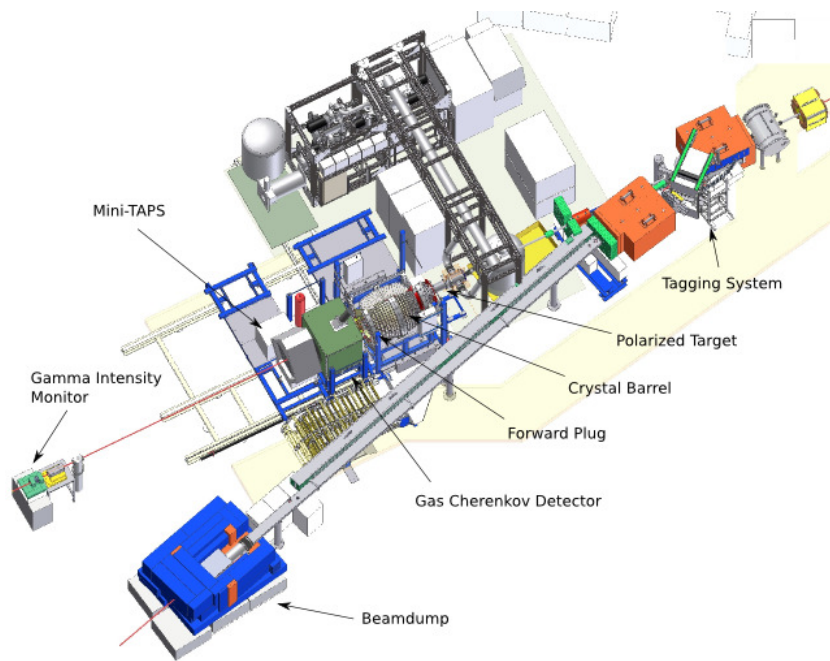


Figure 14: Schematic view of CBELSA experimental setup.

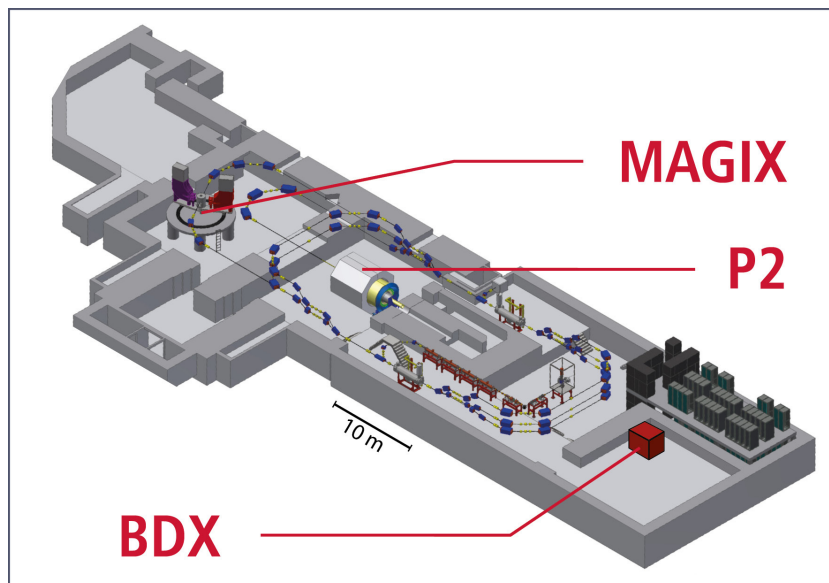


Figure 15: Schematic representation of the MESA accelerator. MAGIX, BDX and P2 are main experimental setups.

Measuring this angle is essential, because it will provide us with information on the fundamental properties of the interactions between elementary particles. In addition, if the weak mixing angle can be precisely measured, it provides insight into other aspects of physics, such as dark matter or hitherto unknown forces in nature.

In the P2 experiment it will be done by measuring the parity violating asymmetry in elastic electron-proton scattering. P2's target relative accuracy of 0.1% exceeds existing measurements in low energy processes by more than one order of magnitude. This increase in accuracy regarding low energy processes is especially important in the search for clues beyond the standard model and can thus supply new evidence beyond the standard model. The P2 experiment can measure the effects of new particles in a range of 50 MeV to 6.4 TeV and is complementary to the direct search for such particles at the LHC. The polarization of the electron beam in this case must be determined with an uncertainty of 0.5%. For this purpose, a new type of Moller polarimeter based on a polarized atomic hydrogen target (Hydro-Moller-Polarimeter) will be used, the most important element of which is a  $^3\text{He}/^4\text{He}$  Dilution cryostat. DLNP JINR made a significant contribution to the preparation of the P2 experiment: in 2022, the necessary cryostat will be developed and manufactured, based on Contract GSI-JINR (Purchase order No. 4500189093, signed 29.04.2020).

## 4 NN-interactions

### 4.1 Motivation

The existence of three-nucleon forces (3NFs) is not doubted both in the standard meson-exchange picture [48] and in chiral perturbation theory [49]. Their strength and detailed structure are still under discussion. Qualitatively, the importance of many-body forces for nuclei was already realized in the early days of nuclear physics [50]. In the 1950s, the pion field theory was extensively used to derive nuclear forces. In this era, there were attempts to derive 3NF on the same footing as NN interactions.

The development of today's most widely used 3NF models began in the 1970s and early 1980s and was based on the work by Fujita and Miyazawa [51]. The Tucson–Melbourne (TM) collaboration studied the approach in more detail [48] which led to the widely used TM 3NF.

Around the same time, the Urbana group found, that for a description of saturation of nuclear matter, a short range repulsive interaction is required. The force was then adjusted to reproduce the triton binding energy. This led to a series of 3NF called Urbana. The most up-to-date version is called Urbana-IX [52].

When speaking about NN and 3NF one should keep in mind, that any unitary transformation of the Hamiltonian does not change physics. However, that unitary transformation which relates two two-body interaction potentials, which are equivalent on-shell but different in the off-shell region, generates three-body forces [53].

The modern approach of the Effective Field Theory considers two- and three-nucleon forces jointly, i.e., selfconsistently [54–56]. The last results on theory of NN and 3NF are in the papers [57–60].

Development of chiral effective field theory of interaction between nucleons provides a self-consistent treatment of two-, three- and many-nucleon forces and exchange currents on the basis of symmetries of underlying theory of strong interactions – quantum chromodynamics. This

approach is widely applied for low energy nuclear physics and nuclear astrophysics. Necessary low-energy parameters of the theory have to be extracted from experimental data [61].

Nuclear forces obey a certain hierarchy implying that 3NF effects are much smaller, on average, than 2NF. This can be very nicely demonstrated by the inclusive total np and nd scattering data measured at Los Alamos. First calculations including the 3NF have shown that current models of the 3NF can explain approximately 1/2 of deviation of the calculations from the data. Whether shorter range 3NF can help to resolve this issue needs to be seen in future. These observations demonstrate the need for exclusive measurements which can provide a significantly larger sensitivity to 3NF effects for specific regions in phase space or for other observables than total cross sections [62].

## 4.2 Experiments

In the past decades, detection systems suitable for the study of certain aspects of the dynamics of the three-body systems have been developed at various laboratories. The use of polarized beams and/or polarized targets has been very common in the past two decades. In addition to protons and deuterons, neutron beams have also been extensively used at TUNL, Bonn, Erlangen, PSI, Uppsala, LANSCE and RCNP. The obvious disadvantage of the neutron beam is that it cannot be manipulated in the beam lines so that experiments are more difficult. In contrast to charged particle detectors where efficiencies close to 100% can be achieved, the efficiency of the neutron detectors is generally lower and requires a complicated calibration. All these issues are not particularly a problem in these experimental studies. Moreover the theoretical estimates are model independent since Coulomb distortions are absent when one uses neutron beams.

To measure more complicated spin observables such as spin-transfer coefficients or spin-correlation coefficients, one needs to measure the polarization degree of the outgoing particle in the former case or have a polarized target in combination with a polarized incident beam for the latter case.

The existing database is far from being complete. Most of the data correspond to differential cross sections and nucleon and deuteron analyzing powers. A restricted number of more complicated spin observables such as the spin-transfer coefficients has also been measured.

Many of the current nucleon-nucleon (NN) potential models describe neutron-proton and proton-proton scattering data with remarkable precision. However, when these potential models are used to calculate the binding energy of the triton, the predictions are 500-800 keV below the measured value of 8.48 MeV. Three-nucleon forces (3NF) correct the problem, but do not eliminate discrepancies in other 3-nucleon systems. For example, in Nd elastic scattering, the differential cross section minima are underpredicted by NN interactions starting at 60 MeV and extending to higher energies. Adding the 3NF fills up the minima, but does not eliminate the disagreement. This is known as the Sagara discrepancy [63].

The experimentally established analyzing power ( $A_y$ ) is also 25-30% too small, as calculated from NN potentials in neutron-deuteron scattering at low energies. This is the so-called " $A_y$  puzzle". Reasonable changes in the NN interaction and the inclusion of current three-nucleon forces do not rectify the situation. However, new three body forces which have not yet been taken into account, such as the spin-orbit type, may resolve the disagreement [64]. Finally, in very precise measurements of the nd coherent neutron scattering length [65], it was found

that almost all theories were in disagreement with the experiment. It is clear from these disagreements between theory and experiment that the three body system is not completely well understood and that the current 3NF does not always correct apparent deficiencies in NN interactions.

The spin-dependent cross-section difference,  $\Delta\sigma_L(\text{nd})$ , in the nd total cross section has been shown to be sensitive to the same 3NF components that correct the triton binding energy problem.  $\Delta\sigma_L$  is the difference in the nd total cross section for beam and target spins parallel and anti-parallel to each other, with both spins aligned with the beam momentum axis.  $\Delta\sigma_T$  is similarly defined. Theoretical calculations predict that the Tucson-Melbourne three-nucleon force changes  $\Delta\sigma_L$  by 5-10% [66] from its value calculated using only NN interaction potentials.

The total cross-section difference  $\Delta\sigma_L(\text{nd})$  was measured firstly at TUNL [67] for incident neutron energies of 5.0, 6.9 and 12.3 MeV. The results were compared to the theoretical predictions based on the CD Bonn NN potential calculations, with and without the inclusion of the TM-3NF, "but are not of sufficient precision to distinguish the presence or absence of three-nucleon force contributions to the cross-sections".

### 4.3 Former experiments at Prague

At the Charles University Nuclear Center the measurements of  $\Delta\sigma_L(\text{np})$  and  $\Delta\sigma_T(\text{np})$  were performed using the transmission method, i.e., the relative difference in attenuation of a polarized neutron beam passing through a polarized proton target was measured.

A polarized neutron beam was based on the Van de Graaff electrostatic accelerator HV 2500 of the Nuclear Center, Charles University (now belongs to IEAP CTU), using the reaction  $T(d,n)^4\text{He}$  with a deuteron beam ( $E_d = 1.82$  MeV). To achieve a monoenergetic collimated neutron beam, the associated particle method was used [68]. The transversely polarized neutron beam with an energy  $E_n = (16.2 \pm 0.1)$  MeV was emitted at an angle  $\theta_{lab} = (62.0 \pm 0.7)^\circ$ . The value of neutron polarization was taken from [69] and amounts  $P_n = (-13.5 \pm 1.4)\%$ . To get longitudinal polarization for the  $\Delta\sigma_L$  experiment, spin was rotated with the help of a permanent magnet of 0.5 T m.

For these experiments, the frozen spin polarized target has been developed which includes a stationary cryostat with a dilution refrigerator, a movable magnetic system including a superconducting dipole magnet with a large aperture, a superconducting solenoid and electronic equipment for providing a dynamic polarization and NMR signal detection. The polarized sample of 20 cm<sup>3</sup> in volume contained propanediol with paramagnetic Cr(V) impurity. The maximum obtained polarization was 93% and 98% for positive and negative values respectively. The target temperature in a frozen mode was about 20 mK. Under these conditions the proton spin relaxation was approximately 1000 h for positive polarization and 300 h for negative one (with a holding field of 0.37 T). The important peculiarity of the developed target was a big aperture for scattering neutrons detection (50° in the vertical plane and almost 360° in the horizontal plane). The polarization direction is defined by the orientation of the holding field. A detailed description of the target can be found in [70].

The measured value of the total cross section difference for the transverse polarization is

$$\Delta\sigma_T = (-126 \pm 21 \pm 14) \text{ mb.}$$

The first uncertainty shown is the statistical and the second one is systematic error. For longitudinally polarized beam and target



$$\Delta\sigma_L = (-55 \pm 21 \pm 7) \text{ mb.}$$

A phase-shift analysis has been performed to extract the value of the  ${}^3\text{S}_1 - {}^3\text{D}_1$  mixing parameter  $\epsilon_1$ . The result is

$$\epsilon_1 = (1.36 \pm 0.66)^\circ.$$

The physical results obtained in Prague permit a new view to the earlier data in this energy range. Earlier, experimental results of other authors (Bonn, Erlangen, Triangle Universities) supported the hypothesis on the minimum value of  $\epsilon_1$  in the vicinity of 15 MeV. Our results disproved this, which is in good accord not only with the other experimental data in this energy range, but with model predictions, in particular [71, 72].

## 4.4 Proposed experiments at Prague

Now the PPT has been transformed into the frozen spin deuteron polarized target (DPT). DPT is a facility consisting of a  ${}^3\text{He}/{}^4\text{He}$  dilution refrigerator,  ${}^3\text{He}$  and  ${}^4\text{He}$  pumping system, two superconducting magnets providing longitudinal and transverse deuteron polarizations and a PC-controlled equipment to build-up and measure the target polarization. Deuterated 1,2 propanediol with a paramagnetic Cr (V) impurity having a spin concentration about  $10^{20} \text{ cm}^{-3}$  is used as a target material.

A system providing the microwave pumping of deuteron polarization consists of a microwave generator, a wave guide inside and outside the dilution refrigerator, and a multimode cavity containing the target material. The microwave generator is a 4-mm wavelength oscillator using an ATT diode placed inside the invar cavity, an output power is above 100 mW. A frequency tuning in 73.0-75.5 GHz range is provided by the cavity piston. The frequency modulation of the microwave power is necessary to obtain higher deuteron polarization.

The universal system of polarization measurement was created: PC based Liverpool type Q-meter has been put into operation in order to enlarge a range of nuclei whose polarization can be measured. A polarization value for particles with spin  $I = 1$  can be extracted from the measured intensities of transitions between states with spin projections 1, 0, -1 ( $+1 \longleftrightarrow 0$ ,  $0 \longleftrightarrow -1$ ) using the formula  $P = (r^2 - 1)/(r^2 + r + 1)$  where  $r$  is the ratio of the transition intensities. A total error on the polarization measurement does not exceed 3 – 4%. In Fig.1 a typical NMR spectrum together with the fit is shown. At the top plot the experimental spectrum is given with a linear scale, at the bottom plot the spectrum is linearised with NMR frequency. The maximum deuteron vector polarization achieved was 40%. The DPT was described in detail in [73, 74].

Experience showed, that all components of the polarized deuteron target as well as the accelerator worked well. Unfortunately, the intensity of the neutron beam was not sufficient. The attempts to increase the intensity brought problems in the stability of the measured values, and the systematic error increased. It was suspected that the electronics used is responsible (many old modules are still present in the system). Several measurement runs were performed, in order to diagnose the sources of the measurement instabilities. In these runs, individual parts of data acquisition system were analyzed and as a result, better solution has been found (triggering the time-to-digit converter TDC by the coincidence signal of neutron with alpha particle rather than the alpha-particle itself). This improvement was tested with an accelerator and gave improved results. The systematic errors were lowered and the number of events per second was increased 3-4 times. The second reason for the large uncertainties is the polarization

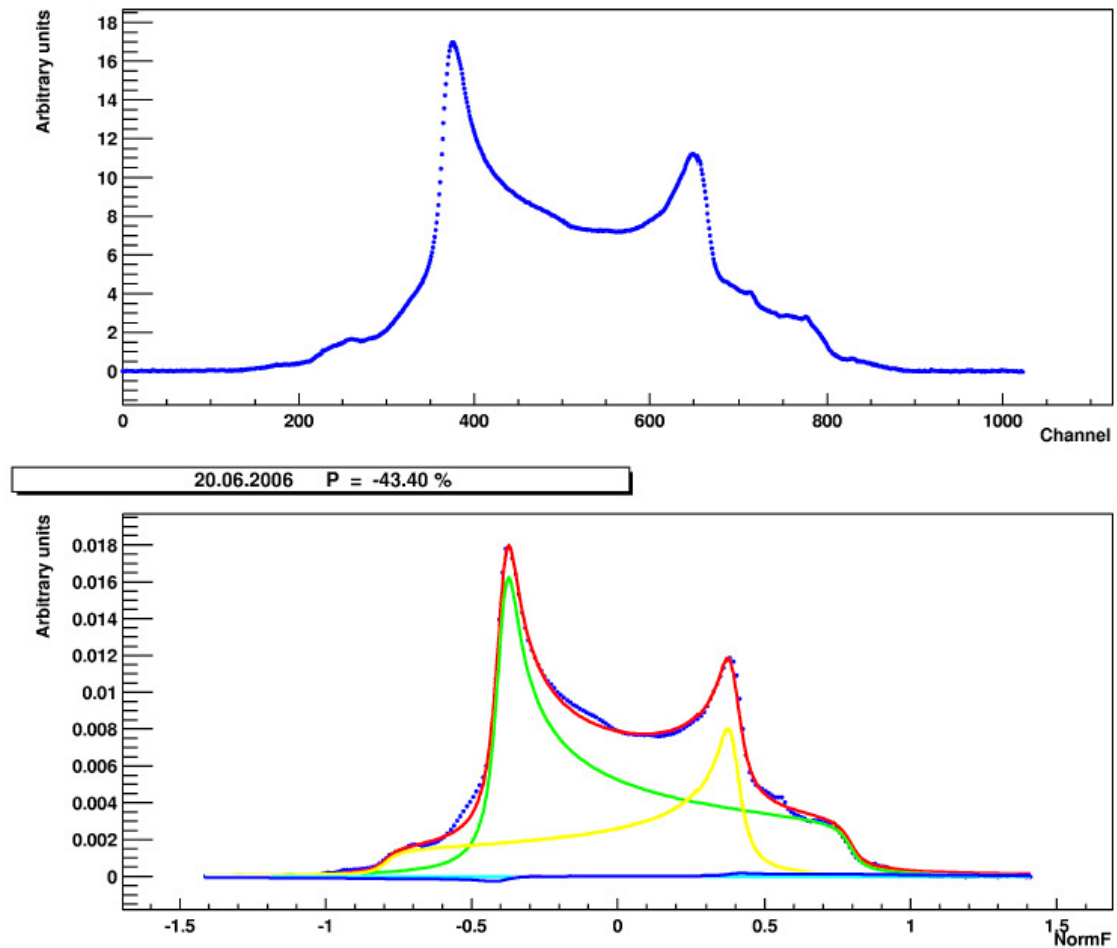


Figure 16: Absorption DMR spectra with the maximum achieved polarization are presented. Top plot: experimental spectrum. Bottom plot: points – experimental spectrum; the components correspond to:  $0 \leftrightarrow -1$  transition (green line),  $1 \leftrightarrow 0$  transition (yellow line), whole DMR spectrum (blue line), sum of the decomposition of a spectrum on the components (red line).

of the deuteron target, which is lower than expected. The average polarization achieved has been  $\simeq 29\%$ .

The last experiments showed that the polarization and intensity of the neutron beam and also the deuteron polarization of the target are insufficient for achieving the necessary accuracy on the measurement of the cross-section difference. Now a modernization of the facility is in progress with the aim to increase the deuteron polarisation of the polarized target and the intensity and polarization of the neutron beam. We will replace our current target material (propanediol) with the novel material, trityl-doped butanol. With this material, polarizations as high as  $\simeq 80\%$  were achieved by the Mainz group [75]. But, in order to use new target materials it is necessary to improve the stability and precision of existing dynamical nuclear polarization apparatus. The linewidth of the resonance of trityl is approximately three times narrower compared to the ones of usually used materials. So we must make a new generator with the required parameters. Also we should test the homogeneity of the superconducting solenoid and correct the field if necessary. The solution to the problem of instability and low statistics would be the increase of the polarisation and intensity of the neutron beam. To improve the parameters of the neutron beam it is proposed to use the reaction  $T(d,n)^4\text{He}$  with polarized deuterons of an energy 100-150 keV. This can be achieved using the known Kaminsky's method [76, 77].

As a first step, it will be production of the polarized deuteron beam with an energy up to 200 keV using channeling of the unpolarized deuteron beam through magnetized Ni film. The electron polarization of the produced deuterium atoms arises from the preferential attachment of electrons of one spin sign. The electron polarization is transferred to the nuclei by the hyperfine interaction. In the ideal case, vector polarisation of deuterons reaches 67% and this polarisation is almost totally transferred to neutrons from the dt reaction.

## 4.5 Polarized deuterons

As to the polarized beam, the first proposal concerning the nuclear polarization via a pick-up of polarized ferromagnetic electrons was made by Zavoiskii in 1957 [78]. The method proposes adiabatic transition of atoms from a high magnetic field to a low magnetic field on the order of 1 mT where nuclei are polarized through the hyperfine interaction.

In Kaminsky's setup a beam of deuterons with a half angle of  $0.01^\circ$  was incident on a Ni(110) foil  $\approx 2\mu\text{m}$  thick within  $0.1^\circ$  of the [110] direction (the critical acceptance angle  $(1.6 - 1.8)^\circ$ ). This is a hyperchanneling regime. He obtained 500 nA/cm<sup>2</sup> of channeled deuterium atoms with an energy of 100-200 keV with nuclear polarization  $P_{zz} = -0.32 \pm 0.010$  (without a significant lattice damage for 25 h of operating time). To test Zavoiskii's proposal Kaminsky passed deuterons through magnetized polycrystalline foils and observed no significant tensor polarization (i.e.  $P_{zz} \approx 0$ ).

Feldman et al. [79] also made polarization measurements with an experimental arrangement very similar to that of Kaminsky. Their data qualitatively agree with Kaminsky's data ( $P_{zz} = -0.14 \pm 0.06$ ). Also, as in Kaminsky's experiment, no effect was seen for polycrystalline foils. In addition, these authors attempted to observe an effect using thin polycrystalline foils of Fe. No effect was seen, possibly because of the presence of fairly thick (50-100 Å) surface oxide layers.

Quite a different electron field-emission experiment [80] on Ni showed that electrons emitted

along the [100], [110] and [137] directions had predominantly spin-up (along the magnetic field), but when emitted along the [111] direction they had a spin-down.

Rau and Sizmann [81], who also used the  ${}^3\text{H}(\text{d},\text{n}){}^4\text{He}$  reaction, measured polarization of the nuclei in neutral deuterium atoms created by electron capture during reflection of a 150-keV  $\text{D}^+$  beam incident at glancing angles ( $< 0.4^\circ$ ) on the surface of magnetized Ni crystals.

The results show that the electron spin orientation is predominantly parallel to the magnetizing field for electrons in the (100), (110), and (111) surfaces and antiparallel in the (120) surface. In the (110) surface the electron polarization is  $P = 96\%$  [82]. This explains the high polarization in Kaminsky's experiment.

On the other hand, there is evidence for polarization of  $1s$  electrons ( $P_{1s} = 0.10 \pm 0.03$ ) attached to F ions as they emerge from magnetized polycrystalline Fe layers [83].

It was found that a vacuum of  $2 \times 10^{-8}$  Torr was necessary in order to see polarization effects. If the vacuum was allowed to deteriorate to  $5 \times 10^{-6}$  Torr, the polarization gradually vanishes, presumably as a result of the build-up of thin layers of surface contaminants.

Ebel [84] tried to explain the high observed polarization by postulating that once a deuteron has captured a spin-up electron inside the crystal, the probability of its losing this electron would be small since the spin-up 3d-band states are filled. A captured spin-down electron, on the other hand, could readily be lost since the spin-down 3d-band states in the crystal are not filled. This would give rise to a pumping of electrons from spin-down to spin-up atomic states of deuterium.

Brandt and Sizmann [85], however, pointed out that stable bound electronic states could not exist in deuterium atoms passing through metals at these velocities. They proposed instead that the electron capture took place in the tail of the electron density distribution at the crystal surface where the density was low enough for bound states to be stable.

Later, Kreussler and Sizmann [86] discussed that at high energies (more than 250 keV/amu) neutralization took place chiefly in the bulk of the crystal and the surface effects were important at lower energies.

## 4.6 Experimental setup

The scheme and photo of the experimental setup is shown in Figs.17, 18. We propose to apply the Sona method, zero-field transitions with total transfer of the electron polarization to deuterons in the atomic beam [87]. We use two permanent magnets ( $2 \times 20$  cm) with a changing distance between the poles ( $B_{\text{max}} = 0.08$  T). The charged deuterons are deflected by the magnetic and electric fields. The Ni foil and the target of a polarimeter are placed in oppositely directed magnetic fields.

The magnetic field is directed along the foil plane (vertically), and we must use Sona transitions with vertical magnetic fields. This is different from the standard configuration.

The single-crystal nickel foils of thickness up to  $2 \mu\text{m}$  are grown epitaxially on NaCl crystals cleaved to expose the (110) plane (produced by Princeton Scientific Corp.). The substrate was dissolved by water and the Ni foils were floated on the Cu disc mounted on the goniometer.

Vacuum of better than  $10^{-4}$  Pa was used.

The atomic beam in a strong magnetic field has vector polarization of deuterons up to the theoretical limit  $P_3 = 2/3$  and zero tensor polarization.

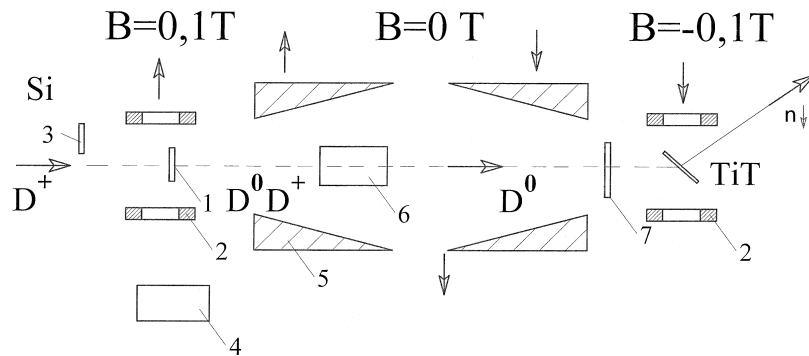


Figure 17: Scheme of the polarized deuteron source; 1 – nickel foil, 2 – permanent magnet (0.07 T), 3 – solid state detector, 4 – a goniometer, 5 – polarizing permanent magnets (for the Sona transitions), 6 – electrostatic plates, 7 – the target of a polarimeter.

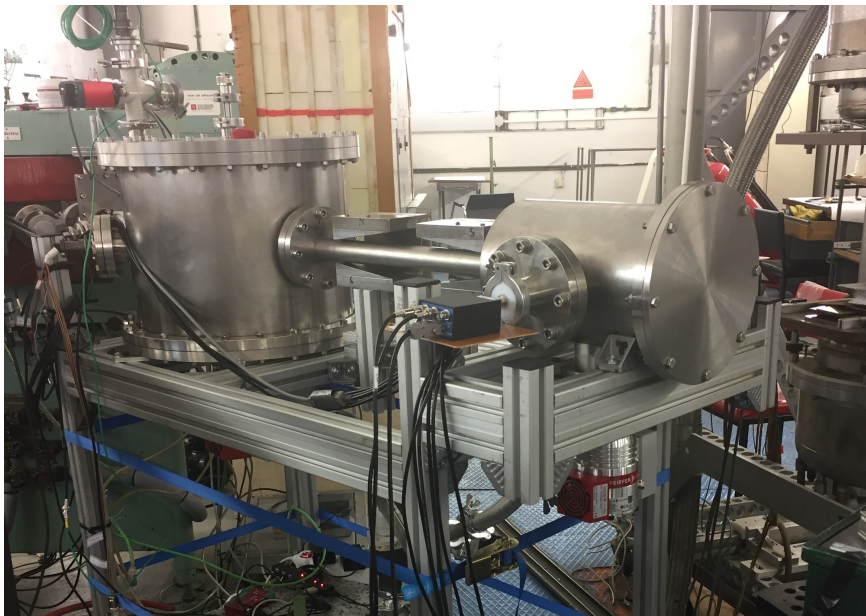


Figure 18: Photo of the experimental setup.

If we pass the deuterium beam to a tritium target, 14-MeV neutrons of the  $dt$ -reaction produced at an angle of  $90^\circ$  (center of mass) have almost the same vector polarization as the deuterons [88].

The deuteron vector polarization may be measured using the reaction  $D(d, p)T$  [89]. The polarimeter target consisted of deuterated polyethylene with a thickness of about 2-3  $\mu\text{m}$  on

a Cu support. The protons produced in this reaction were detected by two surface barrier detectors, each having an effective area of 20 mm<sup>2</sup>.

The detectors were placed symmetrically at  $\pm 120^\circ$  with respect to the beam axis, and the solid angle was  $\approx 1$  msr. In order to suppress the elastically scattered deuterons,  $^3\text{H}$  and  $^3\text{He}$ , each detector was masked with a 10- $\mu\text{m}$ -thick aluminum foil.

For a vector polarized beam the particle intensities detected by two detectors placed on the right and on the left of the beam axis are proportional to the cross sections  $\sigma_R(\theta)$  and  $\sigma_L(\theta)$ , respectively,

$$\sigma_R(\theta) = \sigma_{0R}(\theta) \left[ 1 - \frac{3}{2} P_z A_y(\theta) \right] \quad (4)$$

and

$$\sigma_L(\theta) = \sigma_{0L}(\theta) \left[ 1 + \frac{3}{2} P_z A_y(\theta) \right], \quad (5)$$

where  $\theta$  is the angle between the polarization vector and the beam direction, and  $A_y(\theta)$  is the Cartesian analyzing power for the reaction.

Replacing the cross sections by the corresponding right and left detector intensities,  $N_R$  and  $N_L$ , for polarized beam and  $N_{0R}$ ,  $N_{0L}$  for unpolarized beam, we obtain

$$\frac{N_R(\theta)}{N_L(\theta)} \times \frac{N_{0L}(\theta)}{N_{0R}(\theta)} = \frac{1 - 3/2 P_z A_y(\theta)}{1 + 3/2 P_z A_y(\theta)}. \quad (6)$$

Designating

$$\kappa = \frac{N_R(\theta)}{N_L(\theta)} \times \frac{N_{0L}(\theta)}{N_{0R}(\theta)}, \quad (7)$$

one obtains

$$P_z = \frac{1 - \kappa}{3/2(\kappa + 1)A_y(\theta)}. \quad (8)$$

The statistical error is

$$\delta P_z^2 = \frac{16}{9(\kappa + 1)^4 A_y^2} \delta \kappa^2 + \frac{P_z^2}{A_y^2} \delta A_y^2, \quad (9)$$

where

$$\delta \kappa = \kappa \sqrt{\frac{1}{N_R} + \frac{1}{N_L} + \frac{1}{N_{R0}} + \frac{1}{N_{L0}}}. \quad (10)$$

According to the calculations, for the real magnetic field value the tensor polarization after the Sona transitions is not equal zero,  $P_{zz} \approx 0.1$ . In this case we use the general formula [90]

$$\begin{aligned} \sigma(\theta, \phi) = & \left[ 1 + \frac{3}{2} \sin \beta \cos \phi P_z A_y(\theta) - \cos \beta \sin \beta \sin \phi P_{zz} A_{xz}(\theta) \right. \\ & \left. - \frac{1}{4} \sin^2 \beta \cos 2\phi P_{zz} A_{xx-yy}(\theta) + \frac{1}{4} (3 \cos^2 \beta - 1) P_{zz} A_{zz}(\theta) \right], \end{aligned} \quad (11)$$

where  $A_{xx-yy} = A_{xx} - A_{yy}$ .

For a vertically polarized beam ( $\beta = 90^\circ$ ), the reaction protons detected by two detectors, placed at left ( $\phi = 0^\circ$ ) and right ( $\phi = 180^\circ$ ) of the beam axis, are proportional to cross sections  $\sigma_L(\theta)$  and  $\sigma_R(\theta)$ , respectively, where

$$\sigma_L(\theta) = \sigma_{0L}(\theta) \left[ 1 + \frac{3}{2} P_z A_y(\theta) - \frac{1}{4} P_{zz} A_{xx-yy}(\theta) - \frac{1}{4} P_{zz} A_{zz}(\theta) \right], \quad (12)$$

$$\sigma_R(\theta) = \sigma_{0R}(\theta) \left[ 1 - \frac{3}{2}P_z A_y(\theta) - \frac{1}{4}P_{zz} A_{xx-yy}(\theta) - \frac{1}{4}P_{zz} A_{zz}(\theta) \right]. \quad (13)$$

According to Ad'yasevich [91], at 300 keV  $A_{zz} \approx A_{xx-yy} \approx 0$ , at 400 keV  $A_{zz} + A_{xx-yy} \approx 0$  and in this energy range additional terms can be neglected.

For deuteron with an energy of 200 keV the expected count rate is  $\sim 2 \text{ sec.}^{-1}$  per 1  $\mu\text{A}$  of neutral deuterium atoms on the target and  $\sim 10^{17} \text{ cm}^{-2}$  thickness of the target. The range in  $\text{CD}_2$  is 0.4  $\mu\text{m}$ .

In experiments with nonchannelled atoms the statistics was too low to measure the vector polarization. So, we decided to measure the tensor polarization with TiT target as the cross section for the reaction  $\text{T}(d, n)^4\text{He}$  [92] is approximately 200 times higher than for dd-reaction.

The cross section depends on the c.m. angle between the spin and  $\alpha$  particle direction  $\vartheta$  [76]:

$$\sigma(\vartheta) = \sigma_0 \left[ 1 - \frac{1}{4}(3 \cos^2 \vartheta - 1)P_{zz} \right]. \quad (14)$$

For measurements we used two values for  $\vartheta$ :  $\vartheta = 90^\circ$  and  $\vartheta = 20^\circ$ . As a result,  $P_{zz} = -0.12 \pm 0.04$  (theoretical value is  $P_{zz} = -0.33$  at the deuteron energy of 500 keV for the Ni foil thickness 1.5  $\mu\text{m}$  (the deuterium atom energy is 250 keV).

During this experiment the goniometer was at a random position, and we used only the first magnet of the Sona transition system and the detector was at a small magnetic field. Excluding the nonadiabatic transitions this corresponds to electron polarization of the deuterium atoms after the Ni foil  $P_e = 0.36$  in the direction of the magnetic field and to the deuteron vector polarization  $P_d = 0.24$  after the Sona transition system.

It seems possible that the effect of channeling permits to increase the available deuterium current at the target and polarization. The experiments with channeling are in progress.

## 4.7 Neutron beam

If the target material  $\text{TiT}_N$  contains  $N = 1.5$  tritium atoms/titanium atom, then the density of the target material is  $\rho_{\text{TiT}_N} = 0.85\rho_{\text{Ti}}(47.88+3.015N)/47.88 = 4.19 \text{ g/cm}^3$ , where  $\rho_{\text{Ti}} = 4.505 \text{ g/cm}^3$ . The factor 0.85 arises from the 15% expansion which the titanium lattice undergoes during tritiation. The total yield of neutrons per incident deuteron with an energy of  $E_d = 200 \text{ keV}$  is given by integration on the deuteron energy in the target. As a result, the yield is  $Y = 2.4 \times 10^{-5}$  neutrons per one deuteron, or  $1.2 \times 10^7$  neutrons per steradian per one  $\mu\text{A}$  of deuterons, the deuteron range in the target is  $R \simeq 1.3 \mu\text{m}$ , the activity of the TiT target is  $\simeq 0.35 \text{ Ci/cm}^2$ .

M. Kaminsky obtained 0.5  $\mu\text{A/cm}^2$  of channeled deuterium atoms with nuclear spin polarization without a significant lattice damage for approximately 25 h of operation time. At the beam radius of 3 mm we would have  $\simeq 0.14 \mu\text{A}$  of deuterium atoms. With a solid angle  $3 \times 10^{-4}$  the neutron beam would be  $\simeq 6.3 \times 10^2$  neutrons/s.

With the neutron emission angle  $(83 \pm 0.5)^\circ$  the  $\alpha$ -particles associated with these neutrons are emitted at the angles  $(90 \pm 4)^\circ$  for deuteron energies from 25 keV up to 200 keV. This defines the dimension of the  $\alpha$ -particle detector. We can easily cut off the scattered deuteron of 200 keV from the  $\alpha$ -particles with a thin foil.

## 4.8 Statistical error

According to [71, 72] statistical error for  $\Delta\sigma_{L,T}$  may be written as

$$\Delta\sigma_{L,T} = \frac{\ln \xi(\textit{antiparallel}) - \ln \xi(\textit{parallel})}{\omega P_b P_t}, \quad (15)$$

where  $\omega$  – deuteron surface density of polarized target, deuterons/cm<sup>2</sup>,  $P_b$ ,  $P_t$  – the polarization of the beam and target, respectively, and  $\xi = N_{det}/N_{mon}$ , where  $N_{det}$  and  $N_{mon}$  – neutron counting rates of the detector and monitor, respectively. The monitor counts the neutron intensity before the polarized target.

$$\delta(\Delta\sigma) = \frac{\sqrt{2}}{\omega P_b P_t} \times \sqrt{\frac{1}{\bar{N}_{mon}} + \frac{1}{\bar{N}_{det}}}, \quad (16)$$

где  $\bar{N}_{m,d} = \frac{1}{2}(N_{m,d}(\textit{par.}) + N_{m,d}(\textit{antipar.}))$ .

Absolute statistical error is

$$\delta(\Delta\sigma) = \frac{\sqrt{2}}{\omega P_b P_t} \times \sqrt{\frac{1}{\bar{N}_{mont}} + \frac{1}{\bar{N}_{det}}}, \quad (17)$$

where  $\bar{N}_{mon,det} = \frac{1}{2}(N_{mon,det}(\textit{par.}) + N_{mon,det}(\textit{antipar.}))$

For the polarized target (propanediol)  $\omega = 3 \times 10^{-4}$  mbarn<sup>-1</sup>. At  $P_t = 0.8$  и  $P_b = 0.6$ , one obtains  $1/\omega P_b P_t \approx 7 \times 10^3$  mbarn.

If the detector efficiency is  $10^{-2}$ , and solid angle  $10^{-3}$ , then at  $N_{mon} \simeq N_{det} = 15$  neutrons/s to get  $\delta_{stat}(\Delta\sigma) = 10$  mbarn it is necessary  $t = 72$  hours of data taking for two values of polarization sign.

At a neutron energy of 14 MeV  $\Delta\sigma_T \approx -300$  mbarn. Including 3NF decrease the cross section difference [66] to 20 mbarn, so we can detect this difference.

## 4.9 Main results

An experimental setup has been developed to produce the beam of deuterium atoms with energies of 100-300 keV with polarized nuclei and to measure vector and tensor polarizations of deuterons.

For a nonchanneled beam (the goniometer in a random position), the tensor polarization measurements were carried out with a TiT target in the reaction  $T(d,n)^4\text{He}$ . Our result is  $P_{zz} = -0.20 \pm 0.04$ .

1. Yu.A. Plis et al., Research and Development of the Polarized Deuteron Sources for the Van de Graaff Accelerator. Physics of Particles and Nuclei Letters. **16** (2019) 256-263; preprint JINR E13-2018-69. Dubna, 2018; report in SPIN2018, to be publ.

## 5 Working plan: 2023 - 2024 - 2025

SPASCHARM



**2023** Data taking runs will be carried out using a negative particle beam and the Dubna polarized frozen target. Single spin asymmetries will be measured in inclusive production of charged pions. Single spin asymmetries will be measured in inclusive production of  $\rho(770)$ ,  $\omega(782)$ ,  $\eta(958)$ ,  $f_0(980)$ ,  $a_0(980)$ ,  $f_2(1270)$ .

**2024** The possibility to measure the polarization of  $\Lambda$ -hyperon and the alignment of vector mesons will be investigated also.

**2025** Multichannel Cherenkov counters will be added to measure spin effects with K-mesons.

### GDH

**2023** Commissioning of the new frozen spin target for experiments with Crystal Barrel/ELSA facility at the Bonn University.

**2024** Precision large-acceptance measurements of the beam-spin asymmetry for deuteron photodisintegration in the region of the exotic six-quark state  $d^*(2380)$  at the Mainz IKP and the Bonn University.

Creation of the cryostat for electron polarimeter for future Mainz-MESA accelerator.

**2025** Study of the spectrum and properties of the baryon resonances through the measurements of the polarization observables in meson photoproduction at the Mainz IKP and the Bonn University.

Creation of the cryostat for electron polarimeter for future Mainz-MESA accelerator.

### NN

**2023** Experiments on channeling at the stand of the polarized deuteron source.

**2024** Build up of the polarized neutron source on the base of the polarized deuteron source and to join it with the frozen polarized deuteron target. The exact measurement of vector and tensor polarizations of the deuterons. Preparation of special devices for usage of new target material based on Trityl-doped butanol.

**2025** To prepare apparatus for measurements of the neutron polarization via scattering on the  $^4\text{He}$  target.

## References

- [1] A.V. Efremov, in Proc of 15th Intern. Spin Physics Symposium Upton, 2002, p.235.
- [2] D. Drechsel, S.S. Kamalov, L. Tiator, Unitary isobar model - MAID2007, Eur. Phys. J. **A 34** (2007) 69.
- [3] L. Tiator, M. Gorchtein, V.L. Kashevarov et al., Eta and Eta prime Photoproduction on the Nucleon with the Isobar Model Eta MAID2018, Eur. Phys. J. **A 54** (2018) 210.
- [4] H. Yukawa, Proc. Phys. Math. Soc. Japan **17** (1935) 48.
- [5] V.V. Mochalov et al. Int. J. Mod. Phys. Conf. Ser. **40** (2016) 1660106.
- [6] V.V. Abramov et al. Nucl. Instr. and Meth. **A 901** (2018) 62.

- [7] <http://lhcb-public.web.cern.ch/lhcb-public/Welcome.html>.
- [8] V.V. Abramov et al. J. Phys. Conf. Ser. **798** (2017) 012096.
- [9] V.D. Apokin et al., in Proc. of the IV Workshop on high energy spin physics, Protvino (1991) 288.
- [10] V.D. Apokin et al., Russ. J. Phys. Atom. Nucl. **45** (1987) 840.
- [11] E.R. Nocera, Achievements and open issues in the determination of polarized parton distribution functions, Int. J. Mod. Phys. Conf. Ser. **40** (2016) 1660016; arXiv:1503.03518 [hep-ph].
- [12] D. de Florian et al., Phys. Rev. Lett. **113** (2014) 012001.
- [13] E.R. Nocera et al., Nucl. Phys. **B 887** (2014) 276.
- [14] M.E. Beddo et al., Fermilab proposal P838, January 1991.
- [15] N.S. Borisov et al., JINR communications 13-10253, Dubna, 1976.
- [16] N.S. Borisov et al., Sov. Phys. JETP **60** (1984) 1291.
- [17] W. Roberts, T. Oed, Phys. Rev. **C 71** (2005) 055201.
- [18] R. M. Woloshyn, Nucl. Phys. **A 496** (1989) 749.
- [19] S.B. Gerasimov, Physics of Atomic Nuclei **2** (1966) 430.
- [20] S.D. Drell, A.C. Hearn, Phys. Rev. Lett. **16** (1966) 908.
- [21] R.A. Arndt et al., Phys. Rev. **C 66** (2002) 055213.
- [22] D.Drechsel et al., Phys. Rev. **D 63** (2001) 114010.
- [23] A. Fix, H. Arenhovel, Eur. Phys. J. **A 25** (2005) 115.
- [24] S. Sumowigado, T. Mart, Phys. Rev. **C 60** (1999) 028201.
- [25] Q. Zhao, J.S. Al-Khalili, C. Bennhold, Phys. Rev. **C 65** (2002) 032201.
- [26] N. Bianchi, E. Thomas, Phys. Lett. **B 450** (1999) 439.
- [27] J. Ahrens et al., Phys. Rev. Lett. **84** (2000) 5950.
- [28] J. Ahrens et al., Phys. Rev. Lett. **87** (2001) 022003.
- [29] H. Dutz et al., Phys. Rev. Lett. **91** (2003) 192001.
- [30] H. Dutz et al., Phys. Rev. Lett. **93** (2004) 032003.
- [31] D. Drechsel, T.W. Walcher, Rev. Mod. Phys. **80** (2008) 731.

- [32] S. Simula et al., Phys. Rev. **D 65** (2002) 034017.
- [33] M. Bashkanov et al., Deuteron photodisintegration by polarized photons in the region of the  $d^*(2380)$ . Phys.Lett. **B 789** (2019) 7.
- [34] L.V. Fil'kov , V.L. Kashevarov , M. Ostrick, Search for narrow six-quark states in the reactions  $\gamma d \rightarrow \pi\gamma NN$ . arXiv:1310.8228 [nucl-ex]
- [35] A. Thomas et al., Nucl. Phys. **B 79** (1999) 591.
- [36] B.S. Neganov, N.S. Borisov and M.Yu. Liburg, JETP **50** (1966) 1445.
- [37] B.S. Neganov, Vestn. Akad. Nauk SSSR **12** (1968) 49.
- [38] F. Lehar et al., Nucl. Instr. and Meth. **A 356** (1995) 58.
- [39] N.A. Bazhanov et al., Nucl. Instr. and Meth. **A 402** (1998) 484.
- [40] Yu.A. Usov, Nucl. Instr. and Meth. **A 526** (2004) 153.
- [41] C.S. Akondi, N.S. Borisov, G.M. Gurevich, A.B. Lazarev, A.B. Neganov, Yu.A. Usov et al., Measurement of the Transverse Target and Beam-Target Asymmetries in  $\eta$  Meson Photoproduction at MAMI. Phys. Rev. Lett. **113** (2014) 102001.
- [42] J.R.M. Annand, N.S. Borisov, G.M. Gurevich, A.B.Lazarev, A.B. Neganov, Yu.A. Usov et al., First measurement of target and beam-target asymmetries in the  $\gamma p \rightarrow \pi^0 \eta p$  reaction. Phys. Rev. **C 91** (2015) 055208.
- [43] P.P. Martel, N.S. Borisov, G. M. Gurevich, A.B. Lazarev, A.B. Neganov, Yu.A. Usov et al., Measurements of Double-Polarized Compton Scattering Asymmetries and Extraction of the Proton Spin Polarizabilities. Phys. Rev. Lett. **114** (2015) 112501.
- [44] P. Adlarson, N.S. Borisov, G. M. Gurevich, A.B. Lazarev, A.B. Neganov, Yu.A. Usov et al. Measurement of  $\pi^0$  photoproduction on the proton at MAMI C. Phys. Rev. **C 92** No. 2, 024617 (2015).
- [45] M. Martemianov, N.S. Borisov, G. M. Gurevich, A.B. Lazarev, A.B. Neganov, Yu.A. Usov et al., A new measurement of the neutron detection efficiency for the NaI Crystal Ball detector. Journal of Instrumentation JINST, **10** (2015) T04001.
- [46] G.M. Gurevich, A.A. Lukhanin, F. Maas, Yu.A. Plis, A.O. Sidorin, A.V. Smirnov, A. Thomas, Yu.A. Usov. On the feasibility of using an extracted polarized antiproton beam of the HESR with a solid polarized target. XVI International Workshop in Polarized Sources, Targets and Polarimetry. PSTP2015, Ruhr-University Bochum, Germany, 14-18 September 2015, PoS(PSTP2015)043.
- [47] Yu.A. Usov. Frozen spin target developed at Dubna. Hystory and Traditions. XVI International Workshop in Polarized Sources, Targets and Polarimetry. PSTP2015, Ruhr-University Bochum, Germany, 14-18 September 2015, PoS(PSTP2015)021.

- [48] S.A. Coon et al., Nucl. Phys. **A 317** (1979) 242.
- [49] L.J. Friar, D. Huber, and U. van Kolck, Phys. Rev. **C 5** (1999) 53.
- [50] H. Primakoff, T. Holstein, Phys. Rev. **55** (1939) 1218.
- [51] J. Fujita, H. Miyazawa, Prog. Theor. Phys. **17** (1957) 360.
- [52] B.S. Pudliner et al., Phys. Rev. Lett. **74** (1995) 4396.
- [53] W.N. Polizou , W. Glöckle, Few-Body Syst. **9** (1990) 97-121.
- [54] E. Epelbaum, H.-W. Hammer, Ulf-G. Meißner, Rev. Mod. Phys. **81** (2009) 1773.
- [55] L. Platter, Phys. Rev. **C 74** (2006) 037001.
- [56] J. Rotureau et al., Phys. Rev. **C 85** (2012) 034003.
- [57] D.R. Entem et al., Phys. Rev. **C 96** (2017) 024004.
- [58] P. Reinert, H. Krebs, E. Epelbaum, Eur. Phys. J. **A 56** (2018) 86.
- [59] E. Epelbaum et al., Phys. Rev. **C 99** (2019) 024313.
- [60] S. Binder et al., Phys. Rev. **C 98** (2018) 014002.
- [61] Yu.N. Uzikov, Three-nucleon forces and some aspects of nuclear astrophysics, in The Universe Evolution, nuclear astrophysics. Eds. I. Strakovsky, L. Blokhintsev. New York: Nova Science Publisher, Inc., 2013. pp.269-292. ISBN 978-1-62808-547-7.
- [62] Yu.N. Uzikov, On the contribution of three-body forces to Nd interaction at intermediate energies. JETP Lett. **75** (2002)5; Pis'ma v ZHETF , **75** (2002) 7.
- [63] H. Witala et al., Phys. Rev Lett. **81** (1998) 1183.
- [64] D. Huber, J.L Friar, Phys. Rev. **C 58** (1998) 674.
- [65] T.C. Black et al., Phys. Rev. Lett. **90** (2003) 192502.
- [66] H. Witala et al., Phys. Lett. **B 447** (1999) 216.
- [67] R.D. Foster et al., Phys. Rev. **C 73** (2006) 034002.
- [68] I. Wilhelm et al., Nucl. Instr. & Meth. **A317** (1992) 553.
- [69] M. Koch et al. Nucl. Phys. Spring Meeting, Salzburg, 1992.
- [70] N.S. Borisov et al., Nucl. Instr. & Meth. **A 345** (1994) 421.
- [71] J. Broz et al., Z. Phys. **A 35** (1996) 401.
- [72] J. Broz et al., Z. Phys. **A 359** (1997) 23.

- [73] N.S. Borisov et al., Nucl. Instr. & Meth. **A 593** (2008) 177.
- [74] Yu.A. Usov. Frozen spin target developed at Dubna. History and Traditions. XVI International Workshop in Polarized Sources, Targets and Polarimetry. PSTP2015, Ruhr-University Bochum, Germany, 14-18 September 2015, PoS (PSTP2015) 021.
- [75] S.T. Goertz et al., Nucl. Instr. & Meth. **A 526** (2004) 43.
- [76] M. Kaminsky, Phys. Rev. Lett. **23** (1969) 819.
- [77] M. Kaminsky, in Proc. of 3rd Int. Symp. on Polarization Phenomena in Nuclear Reactions, Madison, 1970, p. 803.
- [78] E.K. Zavoiskii, J. Exp. Theor. Phys. **32** (1957) 408; english translation, Sov. Phys. – JETP **5** (1957) 338.
- [79] L.C. Feldman et al., Radiation Effects **13** (1972) 145.
- [80] W. Gleich et al., Phys. Rev. Lett. **27** (1971) 1066.
- [81] C. Rau, R. Sizmann, Phys Lett. **A 43** (1973) 317-318.
- [82] C. Rau, J. Magnetism and Magnetic Materials. **30** (1982) 141-174.
- [83] K.-H. Speidel et al., Phys. Rev. Lett. **61** (1988) 2616-2619.
- [84] M.E. Ebel, Phys. Rev. Lett. **24** (1970) 1395.
- [85] W.Brandt and R. Sizmann, Phys. Lett. **A 37** (1971) 115.
- [86] S. Kreussler, R. Sizmann, Phys. Rev. **B 26** (1982) 520-529.
- [87] P.G. Sona, Energia Nucleare. **14** (1967) 295-299.
- [88] G.G. Ohlsen, Rep. Progr. Phys. **35** (1972) 717.
- [89] A.A. Naqvi, G. Clausnitzer, Nucl. Instr. & Meth. **A 324** (1993) 429.
- [90] G.G. Ohlsen, P.W. Keaton, Nucl. Instr. & Meth **109** (1973) 41.
- [91] B.P. Ad'yasevich, V.G. Antonenko, V.N. Bragin, Ya. Fiz. 1981. **33** (1981) 1167-1171; english translation: Physics of Atomic Nuclei **33** (1981) 313.
- [92] A. Galonsky et al., Phys. Rev. Lett. **2** (1959) 349.

The project includes 21 participants from JINR. Authors of the project have publications at least on one part of the Project.

### Form No 26

Proposed schedule and necessary resources for realization of the project "SPASCHARM-GDH-NN" (k\$)

Title of expense item	Total cost	Laboratory proposal for distribution of finances		
		2023	2024	2025
1. The modification of the UHF system of the polarized target	15.0	9.0	2.0	4.0
2. Design and preparation of the parts of "Active Target"	6.0	4.0	2.0	-
3. Modification of the polarization measurement system	4.0	2.0	2.0	-
4. Purchase of standard devices	41.0	16.0	14.0	11.0
Total (equipment)	66.0	31.0	20.0	15.0
Materials	26.0	10.0	8.0	8.0
<b>TOTAL</b>	<b>158.0</b>	<b>72.0</b>	<b>48.0</b>	<b>38.0</b>
<b>Finance sources</b>				
Budget expenses				
a) direct (immediate)	201.0	71.0	65.0	65.0
b) grant of Germany (BMBF)	30.0	10.0	10.0	10.0
c) grants of CR	54.0	18.0	18.0	18.0
<b>Total immediate expenses</b>	<b>285.0</b>	<b>99.0</b>	<b>93.0</b>	<b>93.0</b>

Table 4:

Leaders of the Project      A. Kovalik, Yu.A. Usov

## Form No 29

Estimate of the expenses for the Project "SPASCHARM-GDH-NN" (k\$)

	Title of expense item	Total cost	2023	2024	2025
1	R & D agreement expenses	12.0	8.0	2.0	2.0
2	Job cost at the LNP's experimental shop	3.0	1.0	1.0	1.0
3	Materials	66.0	22.0	22.0	22.0
4	Transport expenses	4.5	1.5	1.5	1.5
5	Unforeseen expenses	6.0	2.0	2.0	2.0
6	Electronic instruments	45.0	15.0	15.0	15.0
6	Annual contribution to "A2" -collaboration	24.0	8.0	8.0	8.0
7	Travel expenses	124.5	41.5	41.5	41.5
	inclusive				
	a) to nonruble zone countries	108.0	36.0	36.0	36.0
	b) to ruble zone countries	12.0	4.0	4.0	4.0
	c) visits to JINR	4.5	1.5	1.5	1.5
	Total immediate expenses	285.0	99.0	93.0	93.0

Table 5:

Leaders of the Project            A. Kovalik, Yu.A. Usov

Director of the Laboratory       V.A Bednyakov

Assistant director on finance    G. A. Usova